Acta Geodyn. Geomater., Vol. 22, No. 3 (219), 347–366, 2025
DOI: 10.13168/AGG.2025.0024
journal homepage: https://www.irsm.cas.cz/acta

ORIGINAL PAPER

EVALUATION OF THE DEPOSITIONAL ENVIRONMENTS AND THE SPATIAL VARIATIONS OF GRAIN SIZE CHARACTERISTICS OF RAMGANGA RIVER SEDIMENTS, INDIA

Rayan KHALIL [1], Ahmad F. TURKI [2, 3] and Mohd Yawar Ali KHAN [4], *

[1] *Department of Petroleum Geology and Sedimentology, Faculty of Earth Sciences, King Abdulaziz University, Jeddah 21589, Saudi Arabia*
[2] *Department of Electrical and Computer Engineering, King Abdulaziz University, Jeddah, Saudi Arabia*
[3] *Center of Excellence in Intelligent Engineering Systems (CEIES), King Abdulaziz University, Jeddah, Saudi Arabia*
[4] *Department of Hydrogeology, Faculty of Earth Sciences, King Abdulaziz University, Jeddah 21589, Saudi Arabia*

**Corresponding author's e-mail:* makhan7@kau.edu.sa

ARTICLE INFO

Article history:
Received 22 April 2025
Accepted 21 July 2025
Available online 13 August 2025

Keywords:
Sediments
Grain size
Environment
Linear discriminant function
Passega diagram
Ramganga River

ABSTRACT

There has been an increased interest in erosion processes and the transportation of materials by rivers due to their importance in land utilization and environmental considerations. Evaluating sediment yield and grain size is essential for examining sediment erosion rates, designing reservoirs and dams, predicting the effects of anthropogenic activities and climate change on river systems, and understanding the occurrence of heavy and trace metal contaminants and micropollutants. In this study, twenty-seven samples of bed sediments were obtained from the main channel of the Ramganga River and its tributaries. The sediments were further filtered via a series of stacked sieves with different mesh sizes along with a receiving pan. Each particle size fraction in every sieve, including the pan, was collected, weighed, and noted to identify the hydrodynamic conditions and depositional environments using bivariate plots, linear discriminant function (LDF), and a Passega diagram. The results indicate that the studied sediments exhibit unimodality, with only two bimodal samples in the midstream region. Folk's classification system categorizes the samples into four distinct classes: coarse sand, medium sand, fine sand, and very fine sand, with proportions of 4 %, 33 %, 52 %, and 11 %, respectively. The findings indicate that the upstream samples exhibit the coarsest particle size, are poorly sorted, and are transported through rolling mechanisms. The midstream and downstream samples are finer in size, well sorted, and carried by higher levels of suspension.

1. IINTRODUCTION

Sediments comprise rocks that experience chemical and physical weathering, leading to unconsolidated and loose particles. The particles are degraded and later conveyed to another location. The primary mode of transportation is aquatic movement in ocean currents, rivers, and similar bodies of water. Infrequently observed modes of transportation encompass winds, movements of mass, and glaciers, including landslides. River sediments consist of rock and soils derived from sedimentary, igneous, or metamorphic rocks that have undergone erosion near the surface. Some rocks are readily eroded, whereas others, particularly metamorphic and igneous rocks, are affected by streams only when their surfaces experience alteration (Joshua and Oyebanjo, 2010) – sedimentary rock forms when sediments are deposited and perhaps buried.

A crucial element of river investigation is the examination of bed sediment size and composition. This approach elucidates several river processes, including flow dynamics, hydraulics, geomorphology, pathogen contamination, and reservoir siltation. Several studies have been undertaken on this subject, including (Slattery and Burt, 1997; Pandey et al., 2002; Xu, 1999; Wang et al., 2008; Zhang et al., 2006; Lindholm, 1987; Milliman and Meade, 1983; Gaillardet, 1999; Chakrapani, 2005; Goni et al., 2006; Feng et al., 2011). Pindi and Jayakumar (2023) found that river sediment, which has diverse mineral compositions and particle sizes, significantly influences the hydraulic roughness of the channel bed, impacting turbulence and flow velocity profiles. Sok et al. (2020), studying the Mekong River, emphasised that sediment- a crucial component of fluvial ecosystems- greatly affects river flow dynamics, including flow resistance, channel shape, and ecosystem health. Nwineewii et al. (2018) analysed the ecological risk, concentration, and enrichment factors of specific heavy metals in sediments from Nigeria's New Calabar River. They noted that heavy metals accumulating in the environment pose risks due to bioaccumulation potential and persistence. A study by Ahamad et al. (2024) on Pakistan's River Ravi indicated these metals can enter the food chain and threaten human health. Ren et al. (2018) explored the factors leading to sediment buildup in Wanjiazhai Reservoir, concluding that the process is complex and

Cite this article as: Khalil R, Turki A F, Khan MYA: Evaluation of the depositional environments and the spatial variations of grain size characteristics of Ramganga River sediments, India. Acta Geodyn. Geomater., 22, No. 3 (219), 347–366, 2025. DOI: 10.13168/AGG.2025.0024

governed by various parameters, especially the grain size distribution of incoming sediments. Numerous elements affect the sediment load and grain size characteristics of a river, such as basin area, lithology, discharge, climatic conditions, topography, anthropogenic activities, and river energy. These aspects have been thoroughly examined by academics, including in (Xu et al., 2012; Weltie and von Eynatten, 2004; Walling, 2005; Warren et al., 2003; Boggs, 2006; Khan et al., 2017; Khan et al., 2024; Panwar et al., 2024; Panwar et al., 2020). In mountainous areas, river energy is the principal factor influencing grain size and sediment load. These components vary temporally and spatially, affected by slope, rainfall patterns, discharge, and other related variables. The dimensions of grains markedly affect the chemical composition of sediments, leading to the preferential accumulation of specific components within various particle size fractions (Lindholm, 1987; Xu et al., 2012; Yadav et al., 2024). Walling (2005) and Warren et al. (2003) have underscored the importance of fine sediment in the transport of nutrients, pathogens, contaminants, and heavy metals within river systems.

Granulometric evaluation is generally performed to evaluate the extent of resistance to external factors influencing the flow of bed sediment along the grain. Provenance-related processes, including erosion, abrasion, deposition, weathering, and transportation, are crucial in formulating an interpretation. The resistance level of a rock can be assessed by examining its grain size. Exogenic processes alter the size and morphology of sediment particles. Precipitation occurs due to the movement of the main agents, including water and sediment grains, as evidenced by deposition and transport processes. According to Daityari and Khan (2017), the dimensions of grains in sedimentary rocks are affected by transport mechanisms, variations in sediment grain size, and energy deposition. The data acquired from sediment grain size measurements are employed to precisely determine these three processes.

Numerous scholars have examined various aspects of the Ramganga River (Khan et al., 2017; Khan et al., 2024; Panwar et al., 2024; Panwar et al., 2020; Yadav et al., 2024; Mukherjee and Deb, 2024), as it is a significant tributary of the renowned Ganges Basin. Grain size is a fundamental characteristic of sediment particles. It influences their entrainment, transport, and deposition, offering essential insights into sediment provenance, transportation history, and depositional environments. Few studies have addressed the grain size features of the Ramganga River (Daityari and Khan, 2017) and none have thoroughly examined the depositional environment. Therefore, this study aims to investigate the spatial variation in grain size characteristics of bed sediments to explain the depositional environments of the sediments and understand the mode of transportation and hydrodynamic conditions. To the authors' knowledge, this work is the first to elucidate geographical differences in grain size features and their depositional environments in depth.

2. STUDY AREA

The Ramganga River is a significant tributary of the Ganges River. It emanates from Dudhotali Mountain in India, 2926 m above sea level. It constitutes 8 % of the total catchment area of the Ganges Basin, with a catchment area of 22,685 km². The Ramganga River flows across readily erodible metabasic rocks, quartzites, and dolomitic limestones in the Himalayan region. At the same time, the Quaternary lithostratigraphic sequence incorporates both recent and ancient alluvium in the Ganga flood plains (GFP) (Khan et al., 2016). The river extends a total length of 642 km from its origin to its confluence with the Ganges. It joins the GFP in Kalagarh after traversing 158 km in the hilly region (Khan et al., 2019). The impressive Ramganga reservoir has been constructed in this location (CWC, 2012; Khan et al., 2017; Gupta and Joshi, 1990). The river traverses extensively industrialized and agriculturally intensive areas inside the densely populated cities of Uttar Pradesh in the GFP, such as Bareilly, Rampur, Bijnor, Moradabad, Hardoi, Farrukhabad, and Shahjahanpur, before draining into the left bank of the Ganges.

2.1. PHYSIOGRAPHY, RELIEF, AND CLIMATE

The horseshoe-shaped pattern of the river in the central and outer Himalayas comprises harsh topography. The southern region of the Himalayan hills encompasses a portion of the basin area known as the Siwalik Hills. Its narrow valleys and steep slopes characterize the basin. The Ramganga River demonstrates considerable variations because of disparities in slope and elevation (Fig. 1). The elevation of the river varies from over 2439 m to below 305 m above sea level in the Himalayas and GFP, respectively. The river exhibits a similar degree of slope variation. The river's minimal gradient is represented in GFP, varying from 0 to 5 %, while in mountainous regions, it surpasses 30 %.

The investigated region has three distinct seasons: summer, wet, and winter. The winter season begins in November, following a brief autumn phase that starts in mid-October and is marked by a notable drop in temperature. Figures A1 (a), (b), and (c) illustrate the temporal variations in temperature in the upstream, midstream, and downstream regions of the river (http://indiawaterportal.org/).

Figures A2 (a), (b), and (c) demonstrate that the rainy period begins in mid-June and continues throughout September or mid-October. May/June and October/November are identified as the pre-monsoon and post-monsoon months, respectively. Occasional precipitation is also seen during wintertime periods (http://indiawaterportal.org/). The area receives an average yearly precipitation of around 1000 mm (Khan et al., 2017).

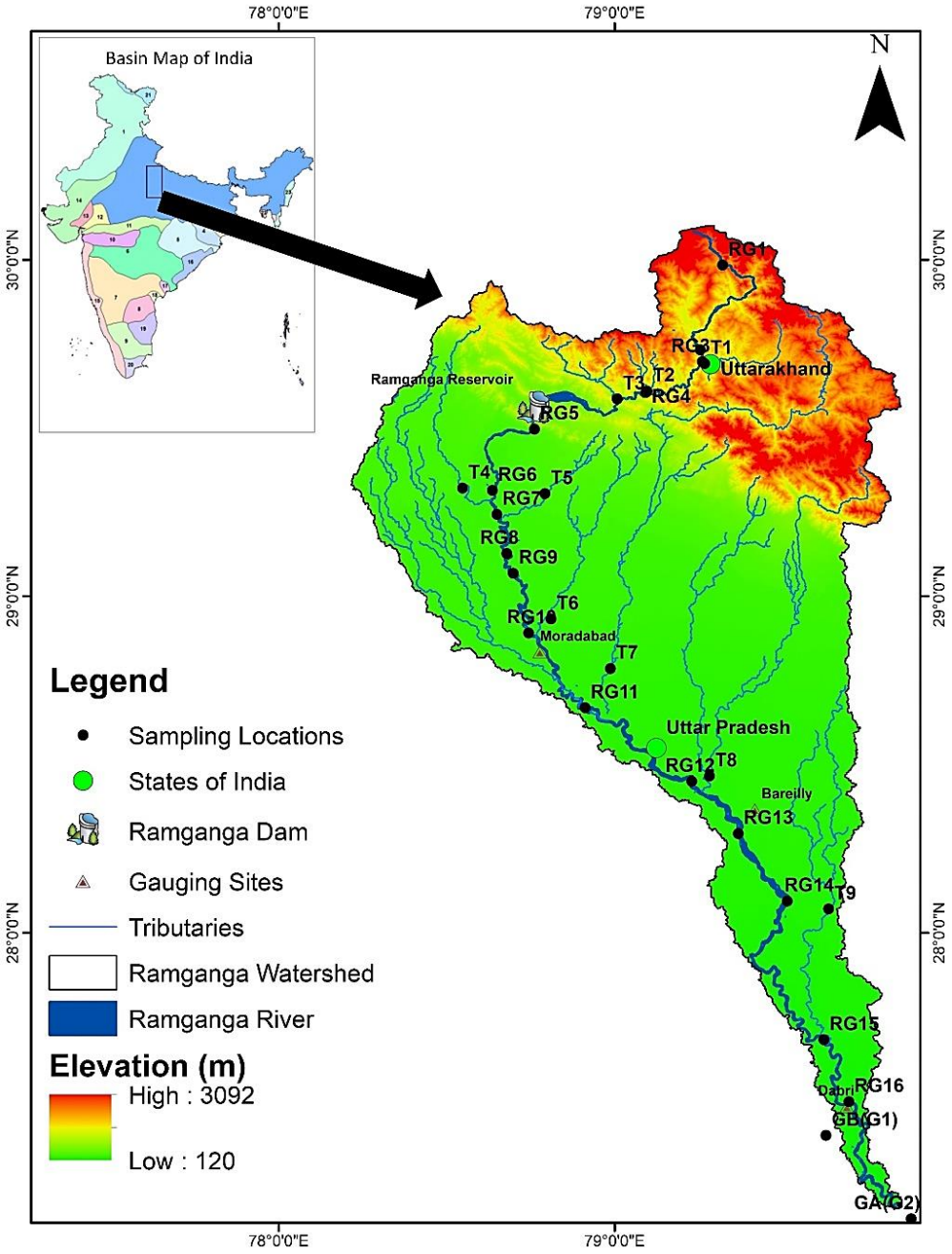

Fig. 1 Ramganga River catchment.

2.2. GEOLOGY OF RAMGANGA RIVER BASIN

The primary lithotectonic zones comprising the entire catchment area are the Lesser and Sub-Himalayas. The primary components of the Sub-Himalayas, which are characterized by molasse deposits from the Pleistocene to Mid-Miocene epochs, comprise sandstone, clay, siltstone, and boulders. Nonetheless, a sequence of unfossiliferous low- to high-grade meta-sediments from the Paleozoic to Mesozoic eras constitutes the predominant geological feature of the Lesser Himalayas (Fig. 2). Sandra and Nagthat formations (Quartzites), Infrakrol/Blaini formations (siltstones and calcareous shales), Deoband and Krol formations (limestones), slates, phyllites, and schists (low-grade metamorphics), and granite gneisses (high-grade metamorphics) constitute the predominant rock types in the catchment (Gupta and Joshi, 1990).

The general strike of the rocks is NW-SE, which is in line with the local Himalayan trend. These have been divided into nappe sheets, and the region contains a number of significant structural/tectonic features, including faults and thrusts. These are characterized by large, linear troughs that have severely crushed and sheared the rock units. Additionally, it is likely that some of these structural characteristics are still moving.

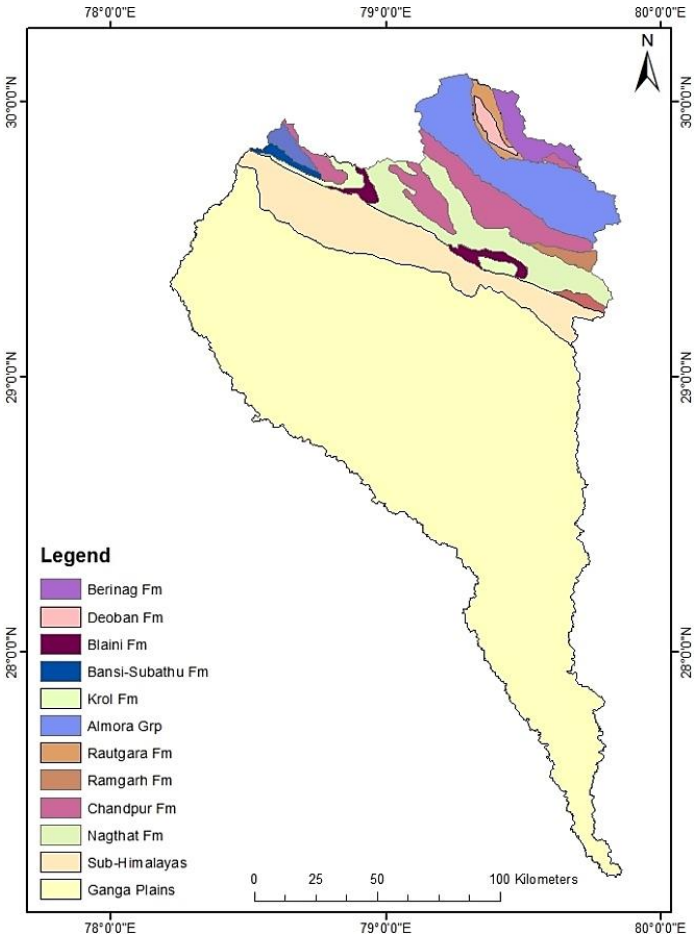

Fig. 2 Lithological map of the study area (modified after Valdiya, 1980).

The river emerges in the GFP after traversing over 158 km through the mountains. The Himalayan orogeny has been closely linked to the GFP, a foreland basin (Fig. A3). (1) The Varanasi Older Alluvium with two facies, namely sandy and silt clay, (2) the Ganga/Ramganga Terrace Alluvium, and (3) the Ganga/Ramganga Recent Alluvium, which together make up the Newer Alluvium, are the units that make up the Quaternary lithostratigraphic sequence in the GFP, which was established in ascending order (Khan and Rawat, 1992).

The Varanasi Older Alluvium represents the most ancient Quaternary formation. It was developed in the Doab of the Ramganga River and the Ganges, which lays unconformably over the Siwalik Supergroup, with a thickness ranging from 300 to 517 meters. The Siwalik Supergroup sediments are situated on the Vindhyan Supergroup's Precambrian basement. It comprises a polycyclic succession of clay, silt, and sand, interspersed with sporadic concretions of Kankar inside silty clay at greater depths. The visible facies of this lithostratigraphic unit consist of medium to fine-grained micaceous deposits of a sandy nature. This facies exhibits oxidation near the surface, presenting a deep brown hue, which transitions to gray at greater depths. As we explore deeper into these sands, sedimentary patterns such as cross-bedding and parallel laminations are evident, indicating a river origin. The silt clay facies exhibit a strong khaki brown hue and may contain Kankar concretions (Khan and Rawat, 1992).

The Ganga Terrace Alluvium, confined to the palaeobanks of the Ganga or Ramganga, has alternating layers of unoxidized gray silty clay and medium to fine sand, with sedimentary formations such as parallel laminations and cross-bedding.

The Ramganga Terrace Alluvium sediments are coarser than those of the Ganga Terrace sands. Well-preserved sedimentary formations have also been identified in these sands. The Ganga/Ramganga Recent Alluvium is confined to the current bank boundaries and comprises medium to fine gray sands, along with thin layers of silt shown as point and channel bars (Khan and Rawat, 1992).

Geomorphologically, the major landforms of the area include (a) an upland—the Bhangar surface or the Varanasi Older Alluvium Plain with two surfaces, i.e., a sandy surface represented by sandy mounds and ridges with sand flats and a silty-clay surface showing a flat topography, and (b) a lowland, the Khadar surface defining the various levels of sand each defined by a bluff. The highest level of terrace in the

Ramganga River and Sot River is an erosional terrace over Varanasi Older Alluvium, followed at a lower level by the Terrace Alluvial plains of the Ganga and Ramganga over the Newer Alluvium and the active flood plain restricted to present-day bank limits and represented by the Recent Alluvium Flood Plain of the river in the form of two to three levels of terraces (Khan and Rawat, 1992).

A basement fault with an NE-SW trend passes near Budaun, which divides the area into a northern uplifted region (Chandausi uplift) and a southern depressed area (Sarda depression). A faulted structure resembling a dome has also been observed near Ujahani according to seismic surveys.

The economic resources of the area are meager and include brick clay, masonry sand, Reh, and promising groundwater potential. The environmental hazards of the area are mainly the alkalinization of soil, annual flooding or low-lying areas, migration of Bhur sand, river bank erosion and river shifting, water logging around depressions, and badland formation along the Sot River (Khan and Rawat, 1992).

3. MATERIALS AND METHODS

There are three types of particle size measurement methods including: measuring particle sizes using the grade scale method; performing quantitative analysis using the statistical and graphical method, and the data genetic method. The most significant method for evaluating depositional environments is the statistical and graphical technique (Boggs, 2012). It includes plotting weight percentage versus particle size in phi (∅) units in addition to calculating statistical particle size parameters, including the inclusive particle size mean, standard deviation, kurtosis, and skewness. Sedimentary environments can be distinguished utilizing bivariate plots of particle size parameters (Friedman, 1961) in addition to log probability diagrams of particle sizes (Milliman and Meade, 1983). Log probability diagrams can also indicate the transportation mechanisms of the sediments, such as traction, saltation, and suspension (Visher, 1969).

Twenty-seven samples of sediments were collected from the main channel of the Ramganga River and its tributaries. Figure 1 and Table A1 show the sample locations. The samples were collected from a 10–15 cm depth by utilizing a stainless-steel spatula and then preserved in clean polythene bags. The samples were dried in an oven at 110 °C for 24 hours. After being removed from the oven, 1000 g of each sample was poured into the appropriately organized set of sieves. The sediments were sieved using a series of stacked sieves with mesh sizes of 1408, 1184, 996, 837, 704, 592, 498, 419, 352, 296, 249, 209, 176, 148, 125, 105, 88, 74, 62, 52, 44, 37, 31, 26, 22, 19, 16, 13, 11, 9, 8, 7, and 6 microns (μm), in addition to a receiving pan. Each sample was poured into the highest sieve and shaken for fifteen minutes. Each fraction of each sieve and receiving pan was collected and weighed.

The particle sizes were converted from millimeters (D) to ∅ units using Equation 1, which was introduced by Krumbein and Monk (1943).

$$\emptyset = -log_2(D) \quad (1)$$

The cumulative percentage was plotted against the particle size in ∅ units to detect the 1st, 5th, 16th, 25th, 50th, 75th, 84th, and 95th percentiles. The particle size parameters were then calculated, including the inclusive graphic mean (M_Z), inclusive graphic standard deviation (σ_I), inclusive graphic skewness (Sk), and graphic kurtosis (K) using Equations 2-5 proved by Folk and Ward (1957) as follows:

$$M_Z = \frac{\emptyset_{16}+\emptyset_{50}+\emptyset_{84}}{3} \quad (2)$$

$$\sigma_I = \frac{\emptyset_{84}-\emptyset_{16}}{4} + \frac{\emptyset_{95}-\emptyset_{5}}{6.6} \quad (3)$$

$$Sk = \frac{\emptyset_{84}+\emptyset_{16}-2\emptyset_{50}}{2(\emptyset_{84}-\emptyset_{16})} + \frac{\emptyset_{95}+\emptyset_{5}-2\emptyset_{50}}{2(\emptyset_{95}-\emptyset_{5})} \quad (4)$$

$$K = \frac{\emptyset_{95}-\emptyset_{5}}{2.44(\emptyset_{75}-\emptyset_{25})} \quad (5)$$

Bivariate plots were generated to differentiate depositional environments based on their particle texture variations. To distinguish between depositional environments, the linear discriminant function (LDF) technique introduced by Sahu (1964) was implemented. The parameters of the grain size analysis, log probability plots, and C-M plots (comparing the one-percentile value to the median) were utilized to differentiate between depositional processes, sedimentation mechanisms, and transportation strategies (Boggs, 2006; Visher, 1969).

The four grain size analysis parameters are defined as follows:

The distribution of sediment particle sizes is described quantitatively by M_Z.

The degree of dispersion of grain sizes from the average size is measured with σ_I, commonly known as grain size sorting.

The quantitative indicator of the degree of symmetry in the grain size distribution is the Sk parameter.

By evaluating the difference in sorting or spreading between the tail spread and the central distribution section, the parameter K measures the degree of sharpness in the grain size frequency curve.

4. RESULTS AND DISCUSSION

4.1. GRAIN SIZE STATISTICS

The distribution of grain sizes is influenced by factors such as lithological composition, climate, weathering intensity, river energy, and basin physiography (Pandey et al., 2002; Xu, 1999; Zhang et al., 2006; Gaillardet, 1999; Sahu, 1964). Climate change, including frequent and severe rainfall events, can exacerbate erosion and sediment influx into rivers, lakes, and streams (Kido et al., 2023; Chalo et al., 2023; Ranjan et al., 2023). These occurrences may

Table 1 Graphic measurements and grain size parameters of the mainstream of the Ramganga River and its tributaries.

Sample	Ø5	Ø10	Ø16	Ø25	Ø50	Ø75	Ø84	Ø90	Ø95	C	Md	Gravel %	Sand %	Mud %
RG1	0.00	0.25	0.47	0.74	1.31	1.90	2.22	2.53	2.94	1,367	406	0.00	99.66	0.34
RG2	0.18	0.50	0.74	0.99	1.44	1.89	2.12	2.36	2.71	1,256	370	0.00	100.00	0.00
T1	0.27	0.54	0.76	0.97	1.41	1.97	2.34	2.68	3.10	1,183	379	0.00	99.59	0.41
RG3	-0.05	0.15	0.34	0.55	0.99	1.41	1.61	1.80	2.09	1,365	505	0.00	100.00	0.00
T2	0.38	0.66	0.87	1.12	1.72	2.39	2.72	3.03	3.47	1,074	304	0.00	98.05	1.95
RG4	0.30	0.54	0.72	0.90	1.27	1.68	1.93	2.20	2.57	1,125	416	0.00	100.00	0.00
T3	0.50	0.77	0.96	1.18	1.67	2.25	2.56	2.84	3.18	1,025	315	0.00	99.57	0.43
RG5	1.76	1.90	2.04	2.18	2.49	2.83	2.99	3.17	3.42	378	178	0.00	99.11	0.89
RG6	1.23	1.37	1.51	1.63	1.92	2.21	2.37	2.49	2.70	536	266	0.00	100.00	0.00
T4	1.33	1.54	1.69	1.90	2.57	3.46	3.81	4.14	4.63	506	169	0.00	87.97	12.03
RG7	1.24	1.46	1.61	1.79	2.17	2.59	2.80	3.09	3.46	612	223	0.00	98.47	1.53
T5	1.48	1.61	1.75	1.88	2.21	2.65	2.91	3.17	3.49	443	216	0.00	98.83	1.17
RG8	0.97	1.19	1.35	1.53	1.90	2.30	2.50	2.73	3.07	726	268	0.00	99.05	0.95
RG9	1.94	2.18	2.37	2.59	3.09	3.69	4.02	4.34	4.75	352	118	0.00	83.75	16.25
RG10	1.54	1.74	1.88	2.06	2.47	2.93	3.18	3.41	3.71	445	181	0.00	97.70	2.30
T6	1.71	1.87	2.02	2.16	2.49	2.84	3.01	3.20	3.44	391	178	0.00	99.14	0.86
RG11	1.66	1.88	2.05	2.23	2.57	2.93	3.11	3.27	3.49	433	168	0.00	99.16	0.84
T7	1.27	1.41	1.55	1.68	2.00	2.34	2.50	2.70	2.95	521	251	0.00	100.00	0.00
RG12	1.50	1.65	1.79	1.94	2.30	2.70	2.91	3.11	3.39	455	204	0.00	99.12	0.88
T8	2.48	2.77	3.00	3.24	3.76	4.42	4.86	5.34	5.97	266	74	0.00	61.36	38.64
RG13	1.29	1.43	1.56	1.70	2.00	2.32	2.48	2.64	2.85	496	251	0.00	100.00	0.00
RG14	1.62	1.82	1.98	2.15	2.56	2.99	3.20	3.40	3.35	412	170	0.00	98.11	1.89
T9	0.89	1.17	1.36	1.58	2.07	2.66	2.97	3.26	3.65	836	240	0.00	97.62	2.38
RG15	2.07	2.37	2.61	2.88	3.46	4.13	4.56	5.04	4.88	347	91	0.00	71.62	28.38
RG16	0.93	1.17	1.35	1.55	1.99	2.54	2.90	3.23	3.64	720	252	0.00	97.92	2.08
GB(G1)	0.52	0.73	0.86	1.02	1.32	1.64	1.79	1.96	2.20	971	402	0.00	99.82	0.18
GA(G2)	1.88	2.08	2.25	2.43	2.92	3.47	3.74	4.00	4.40	342	132	0.00	90.21	9.79

also increase sediment loading due to stormwater runoff. Lithology may influence the modification of hillslope-coupled streams through differential sediment supply and erosion rates. It was found to be the primary factor affecting bankfull sediment concentration, which acts as a proxy for sediment supply, with increased concentrations noted in streams draining softer lithologies, based on a study of 80 streams in the Rocky Mountains, USA (Mueller and Pitlick, 2013). With the increase in turbulent kinetic energy of the stream, the concentration of suspended particles rises, whereas sedimentation diminishes (Tinoco and Coco, 2018; Zhang et al., 2020). The fluctuation in suspending power can elucidate the changes in the silt concentration of rivers. The particle size characteristics were analyzed and interpreted using statistical techniques. The cumulative frequency and histogram plots were generated using the statistical properties obtained from the grain size analysis of twenty-seven sediment samples. These parameters, including M_Z, σ_I, Sk, and K, were calculated using different percentile values, as shown in Table 1.

Parameters including M_Z, σ_I, Sk, and K were derived from graphical representations (frequency curve and histogram). The histogram and cumulative frequency curve (Figs. 3, 4, and A4) illustrate the frequency of particles within each size class and provide a quick representation of the grain size distribution.

Figures 3, 4, and A4 show that all the samples collected from the Ramganga River have unimodal distributions, with peaks ranging from 1.26Ø to 3.76Ø, with the exception of two midstream samples (T4 and RG7), which have bimodal distributions. This is an indication that most of the samples have one source

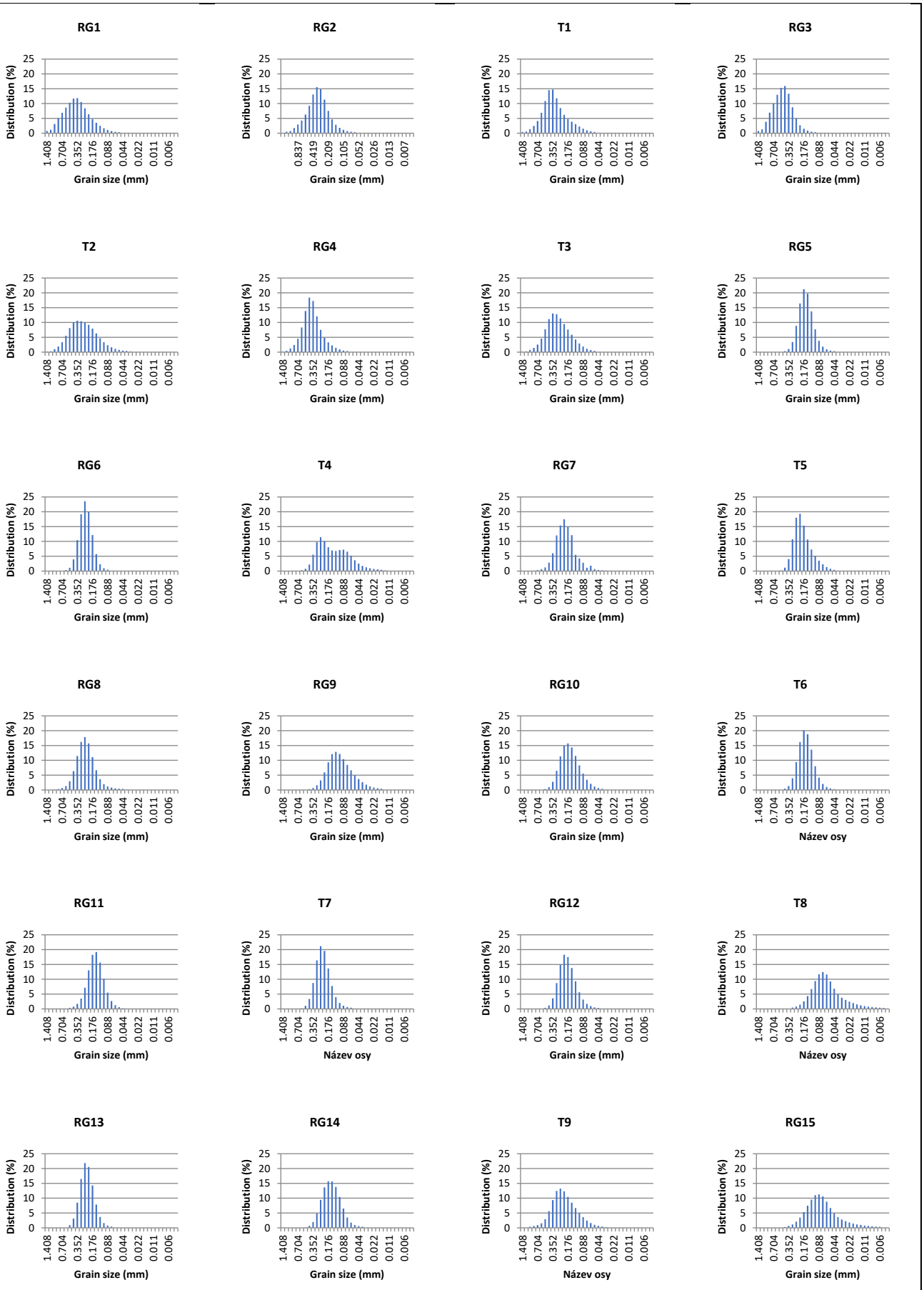
RG1
RG2
T1
RG3
T2
RG4
T3
RG5
RG6
T4
RG7
T5
RG8
RG9
RG10
T6
RG11
T7
RG12
T8
RG13
RG14
T9
RG15
Distribution (%)
Grain size (mm)
Název osy

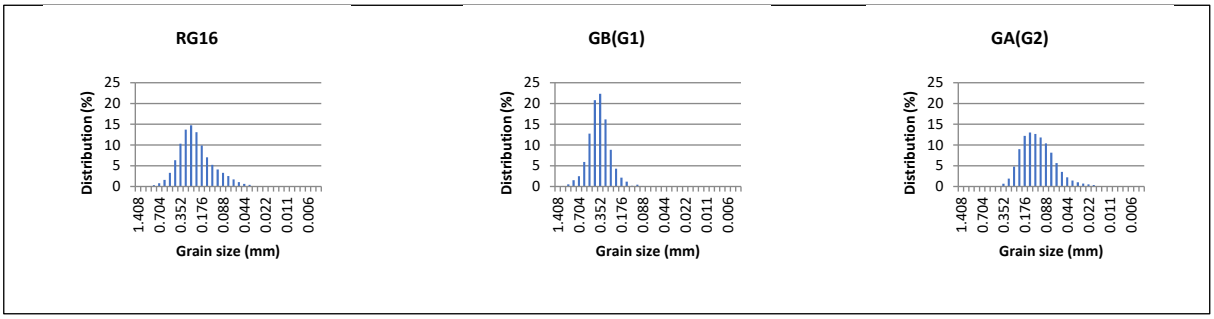

Fig. 3 Frequency plots of the Ramganga River samples.

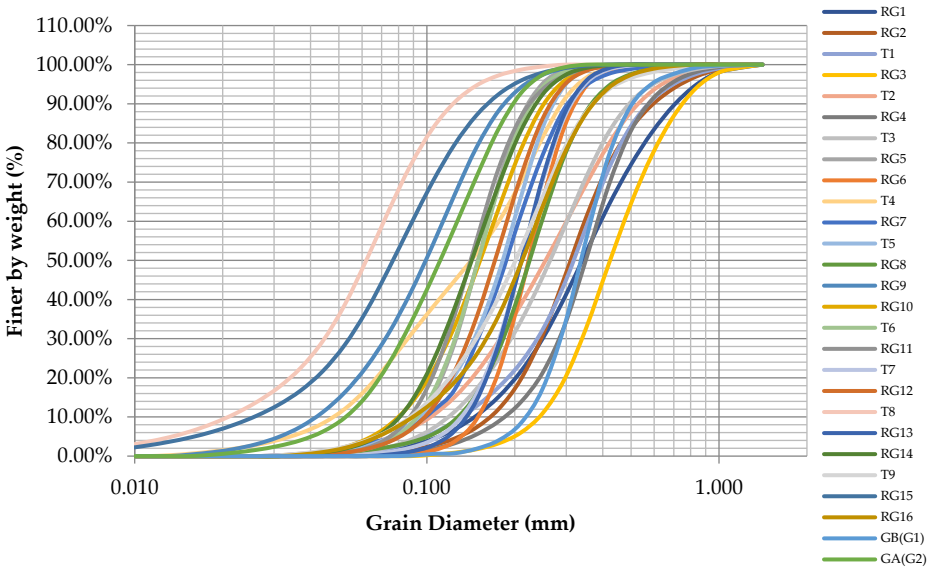

Fig. 4 Cumulative curve of the Ramganga River samples.

and process. The upstream samples peak at 1.51Ø (71 %) and 1.26Ø (29 %). The midstream samples peak at 2.01Ø (33 %), 2.26Ø (25 %), 2.51Ø (25 %), 2.76Ø (14 %), and 3.01Ø (14 %). On the other hand, 38 % of the downstream samples have peaks at 2.01Ø, while the others have variation peaks at 1.51Ø, 2.51Ø, 2.76Ø, 3.51Ø, and 3.76Ø (one sample at each peak).

4.2. GRAVEL, SAND, AND MUD RATIO

The samples were categorized into four distinct classes/facies using Folk's (1957) classification method which include: coarse sand (4 %), medium sand (33 %), fine sand (52 %), and very fine sand (11 %), as shown in Figure 5. Three different categorizations were predicated on the proportional relationships between sand, silt, and mud.

The particle sizes illustrate a wide degree of sorting. By integrating sand, silt, and clay content, the samples can be classified as follows: coarse sand (RG3), medium sand (RG1, RG2, T1, T2, RG4, T3, RG6, RG8, and GB(G1)), fine sand (RG5, T4, RG7, T5, RG10, T6, RG11, T7, RG12, RG13, RG14, T9, RG16, and GA(G2)), and very fine sand (RG9, T8, and RG15). Table 2 illustrates the fractions of the grains within each class.

4.3. GRAIN SIZE PARAMETERS

The following size parameters were determined using the equations of Folk and Ward (1957) and reported using the nomenclature provided by Folk (1966): graphic M_Z, inclusive graphic σ_I, verbal skewness sediments Sk, and verbal sediments K (Table 3). In several areas of research, such as groundwater management and the hydraulic conductivity of sandstone reservoirs, the average size is an important factor. A graphic representation of grain size analysis from coarse to very fine grains indicate a medium-to-low energy depositional environment. A slight variation in grain size indicates modest velocity changes in the depositional medium or a singular source of the particles. Furthermore, Folk and Ward (1957) have shown that grain size exhibits an inverse correlation with grain sorting. Fine-to-medium sand particles exhibit optimal grain sorting,

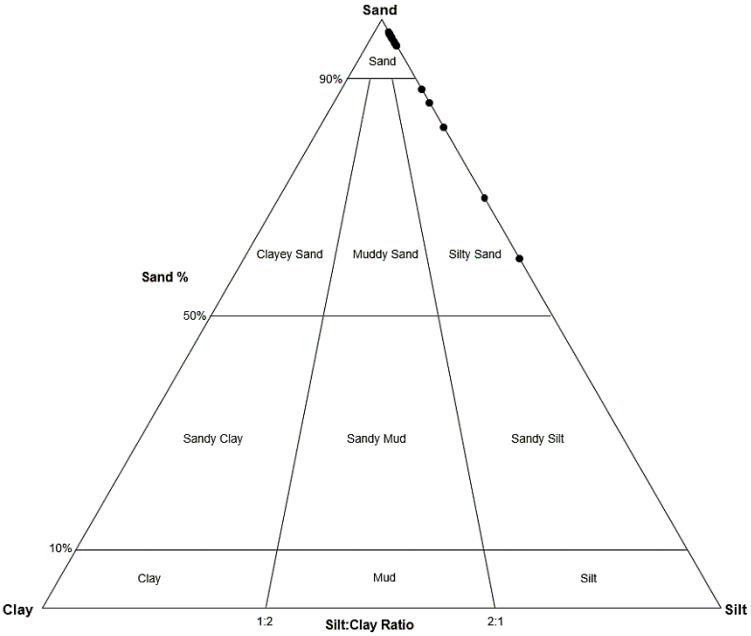

Fig. 5 Grain size distributions of the samples (sand, silt, clay) according to Folk's classification system.

Table 2 Grain size distributions and sediment type according to Folk (1980).

Region	Sample	Gravel %	Sand %	Mud %	Sediment Type
Upstream	RG1	0.00	99.66	0.34	Medium Sand
	RG2	0.00	100.00	0.00	Medium Sand
	T1	0.00	99.59	0.41	Medium Sand
	RG3	0.00	100.00	0.00	Coarse Sand
	T2	0.00	98.05	1.95	Medium Sand
	RG4	0.00	100.00	0.00	Medium Sand
	T3	0.00	99.57	0.43	Medium Sand
Midstream	RG5	0.00	99.11	0.89	Fine Sand
	RG6	0.00	100.00	0.00	Medium Sand
	T4	0.00	87.97	12.03	Fine Sand
	RG7	0.00	98.47	1.53	Fine Sand
	T5	0.00	98.83	1.17	Fine Sand
	RG8	0.00	99.05	0.95	Medium Sand
	RG9	0.00	83.75	16.25	Very Fine Sand
	RG10	0.00	97.70	2.30	Fine Sand
	T6	0.00	99.14	0.86	Fine Sand
	RG11	0.00	99.16	0.84	Fine Sand
	T7	0.00	100.00	0.00	Fine Sand
	RG12	0.00	99.12	0.88	Fine Sand
Downstream	T8	0.00	61.36	38.64	Very Fine Sand
	RG13	0.00	100.00	0.00	Fine Sand
	RG14	0.00	98.11	1.89	Fine Sand
	T9	0.00	97.62	2.38	Fine Sand
	RG15	0.00	71.62	28.38	Very Fine Sand
	RG16	0.00	97.92	2.08	Fine Sand
	GB(G1)	0.00	99.82	0.18	Medium Sand
	GA(G2)	0.00	90.21	9.79	Fine Sand

Table 3 Grain size statistical parameters of the mainstream of the Ramganga River and its tributaries with interpretations.

Region	Sample	M_Z	Sizing	σ_I	Sorting	Sk	Skewness	K	Kurtosis
Upstream	RG1	1.33	MS	0.88	MS	0.1	NSK	1.03	M
	RG2	1.43	MS	0.73	MS	0.0	NSK	1.16	L
	T1	1.50	MS	0.82	MS	0.2	FSK	1.15	L
	RG3	0.98	CS	0.64	MWS	0.0	NSK	1.03	M
	T2	1.77	MS	0.93	MS	0.1	FSK	1.00	M
	RG4	1.31	MS	0.65	MWS	0.1	FSK	1.19	L
	T3	1.73	MS	0.81	MS	0.1	FSK	1.02	M
Midstream	RG5	2.51	FS	0.49	WS	0.1	NSK	1.05	M
	RG6	1.93	MS	0.44	WS	0.1	NSK	1.03	M
	T4	2.69	FS	1.03	PS	0.2	FSK	0.86	P
	RG7	2.19	FS	0.63	MWS	0.1	FSK	1.13	L
	T5	2.29	FS	0.59	MWS	0.2	FSK	1.06	M
	RG8	1.92	MS	0.61	MWS	0.1	NSK	1.12	L
	RG9	3.16	VFS	0.84	MS	0.2	FSK	1.04	M
	RG10	2.51	FS	0.65	MWS	0.1	FSK	1.02	M
	T6	2.51	FS	0.51	MWS	0.1	NSK	1.04	M
	RG11	2.58	FS	0.54	MWS	0.0	NSK	1.07	M
	T7	2.02	FS	0.49	WS	0.1	NSK	1.05	M
	RG12	2.33	FS	0.57	MWS	0.1	FSK	1.03	M
Downstream	T8	3.87	VFS	1.00	MS	0.2	FSK	1.22	L
	RG13	2.01	FS	0.47	WS	0.1	NSK	1.03	M
	RG14	2.58	FS	0.57	MWS	0.0	NSK	0.85	P
	T9	2.13	FS	0.82	MS	0.1	FSK	1.05	M
	RG15	3.54	VFS	0.91	MS	0.1	NSK	0.92	M
	RG16	2.08	FS	0.80	MS	0.2	FSK	1.12	L
	GB(G1)	1.32	MS	0.49	WS	0.0	NSK	1.13	L
	GA(G2)	2.97	FS	0.75	MS	0.1	FSK	0.99	M

Note: M_Z is the graphic mean, σ_I is the graphic standard deviation, Sk is the graphic skewness, K is the graphic kurtosis, CS is coarse sand, MS is medium sand, FS is fine sand, VFS is very fine sand, WS is well sorted, MWS is medium/well sorted, MS is medium sorted, PS is poorly sorted, NSK is near-symmetrically skewed, FSk is fine skewed, M is mesokurtic, P is platykurtic, and L is leptokurtic.

but coarser particles are linked to inferior sorting. The fluctuation in the kinetic energy domain can be elucidated using the standard deviation of the grain size analysis, which signifies the average transportation velocity.

The values exhibit variability among the samples under investigation. Table 3 and Figure 6 show that the sediments of the Ramganga River have M_Z values that range from 0.98 (representing coarse sand) to 3.87 (representing very fine sand), with an average M_Z value of 2.19 (representing fine sand). The σ_I values of the studied samples from the Ramganga River range from 0.44 (well sorted) to 1.03 (poorly sorted), with an average of 2.00 (medium/well sorted). The Sk values of the data span from -0.02 (denoting near-symmetrical skewness) to 0.24 (denoting substantial fine skewness), with a mean of 0.10 (showing fine skewness) (Fig. 6). This variation signifies energy fluctuations within the depositional settings. Folk and Ward (1957) indicated that beach habitats experience frequent waves and current activities, resulting in fine grains and, hence, negative skewness. The positive skewness shows the presence of fine particles, which is characteristic of a fluvial environment. Yang and Shi (2019) asserted that positive skewness may arise from weathering processes that generate fine particles. The kurtosis of grain size distribution indicates the ratio of the core distribution to the tail spread. A beach environment can be classified as leptokurtic; however, Baiyegunhi et al. (2017) asserted that leptokurtic and mesokurtic distributions represent the fine-grained supply following the depletion of sediment transportation energy. The K values span from 0.85, a platykurtic distribution, to 1.22, denoting a markedly leptokurtic distribution, with a mean of 0.95, representing a mesokurtic distribution (Fig. 6). It is worth noting that the upstream samples have medium grain sizes and moderate sorting due to the closer distance from the samples' sources. On the other hand, the downstream samples have finer grain sizes and better sorting due to the long-distance transportation. One reason for this could also be that anthropogenic activities are less common in upstream areas and more frequent in downstream regions. These activities,

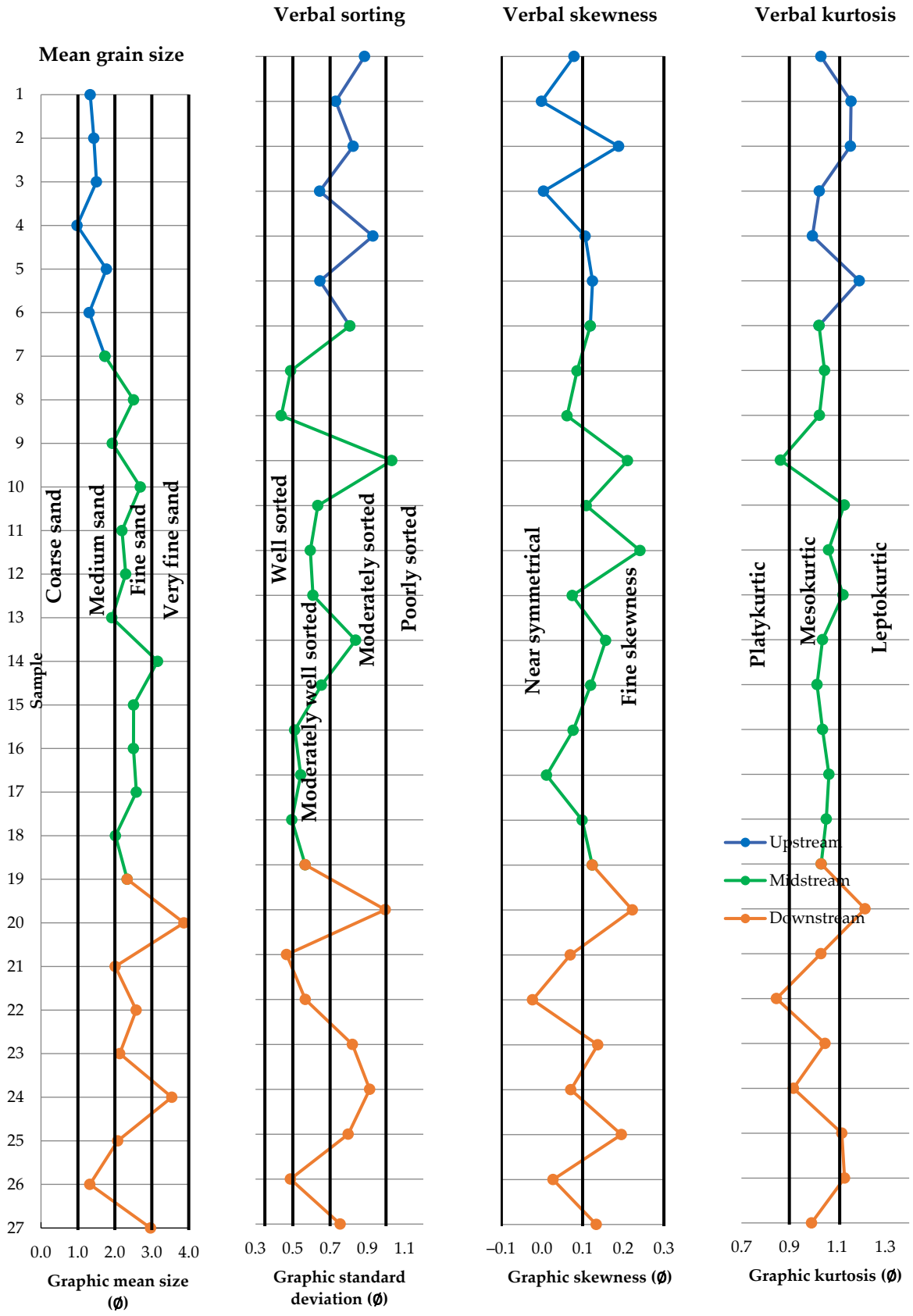

Fig. 6 Textural components of the Ramganga River samples.

including land use changes, dam construction, and industrial discharges, significantly disrupt natural sediment transport and deposition processes, resulting in a noticeable rise in finer sediments downstream of rivers (Zamroni et al., 2020), especially in the Ramganga River's downstream areas, which are increasingly affected by anthropogenic activities (Sarkar et al., 2003; Khan et al., 2016a and b; Khan et al., 2017; Khan et al., 2020).

4.4. LATERAL VARIATION IN SIZE PARAMETERS

Figure A5 illustrates the variance in the size characteristics of the samples taken from the Ramganga River's main channel and its tributaries. There is notable variation in the sediments' M_Z, σ_I, Sk, and K. One possible explanation for the notable variance is the long travel distance (642 kilometers).

4.5. BIVARIATE PLOTS OF STATISTICAL PARAMETERS

The statistical characteristics indicate the sediment transport mechanisms (Folk and Ward, 1957; Singh et al., 2007). Several textural data points are used in bivariate graphs. Several bivariate plots of textural metrics are shown in this work, including mean versus sorting, sorting versus skewness, skewness versus kurtosis, and sorting versus kurtosis, for the sediments of the Ramganga River main channel, as illustrated in Figure 7. The mean size and sorting (standard deviation) values are presented on the bivariate relationship graph. The sediment distribution indicates that the samples vary from coarse sand to very fine sand and exhibit characteristics of extremely poorly to well sorted. The spatial distribution shows that sediment sorting increases downstream of the Ramganga mainstream (Fig. 7a and Fig. 7d). The discontinuities in grain size trends result from tributary inputs and valley-side failures, as indicated by (Knighton, 1980; Dawson, 1988; Rice, 1994; Pizzuto, 1995).

The standard deviation versus mean particle size bivariate plot (Fig. 7a) shows that the upstream sediments are moderately sorted medium sands. Their mean size ranges from coarse sand (0.98) to medium sand (1.77), but on average, they are medium sand (1.44). This is an indication of higher energy levels during the depositional process. On the other hand, the majority of the midstream and downstream sediments are finer in size (fine sand) with better sorting. The mean size of the midstream varies from medium sand (1.92) to very fine sand (3.16), with an average of fine sand (2.39). The mean size of the downstream is close to the midstream, which varies from medium sand (1.32) to very fine sand (3.87), with an average of fine sand (2.56). The sorting of both midstream and downstream is better than the upstream, with an average of 0.62 and 0.73, respectively. This is an indication of lower energy levels during the depositional process.

Skewness quantifies the symmetry of grain size distribution. It signifies the dominance of coarse- and fine-grained sediments in the cumulative frequency curves. The prevalence of coarse-grained sediments in the tail signifies negative skewness, while an abundance of fine-grained sediments in the tail denotes positive skewness (Boggs, 2009). The bivariate plot of the skewness against the mean particle size (Fig. 7b) shows an inverse relationship: when negative skewness (leaning toward fine particles) decreases, the mean particle size increases (decreases in microns). The skewness of the upstream sediments ranges from 0.00 to 0.19∅, with an average of 0.09, indicating near-symmetrical skewness. This is an indication of energy-level stabilization during the depositional process. The midstream and downstream samples have fine skewness, with an average of 0.11 and 0.10, respectively. The kurtosis of the upstream samples has a narrow range from mesokurtic (1.00∅) to leptokurtic (1.19∅), an indication of energy stabilization of the transportation medium. In contrast, the midstream and downstream have a wider variation from platykurtic (0.86∅ and 0.85) to leptokurtic (1.04∅ and 1.22) (Fig. 7c). It is worth noting that this wide variation is another indication of the energy level changing during the deposition process. The positive skewness of these sediments indicates unidirectional channel transit or sediment deposition in a low-to-medium-energy environment (Ramanathan et al., 2009; Hakro et al., 2021). The standard deviation against skewness bivariate plot (Fig. 7d) shows an inverse relationship between particle size sorting and skewness. With a high-energy transport medium, sediments of different sizes are deposited, leading to poor sorting.

Graphic kurtosis quantifies the degree of sorting in the central region of frequency curves, indicating the sharpness of these curves (Fig. 7). The kurtosis of the examined sediments ranges from 0.86 (platykurtic) to 1.22 (leptokurtic) (Table 3). The samples exhibit a range from platykurtic to leptokurtic, with a significant predominance of leptokurtic characteristics (Fig. 7c and Fig. 7e), indicating a periodic variability in the sediment transport agent.

4.6. LINEAR DISCRIMINANT FUNCTION (LDF)

The different procedures and deposition conditions seem to have a substantial correlation with the variations in energy and fluidity characteristics (Sahu, 1964). The deposition method and environment were clarified with Sahu's linear discriminant functions, namely, Y_1 (Aeolian, beach), Y_2 (beach, shallow agitated water), and Y_3 (shallow marine, fluvial). The parameters of grain size analysis, such as M_Z, σ_I, Sk, and K, control all of these functions. The binary plots of linear discriminant functions and the deposition environment are shown in Figure 8 and Table 4.

To discriminate between aeolian and beach, the following equation (Y_1) can be used, with a cutoff of -

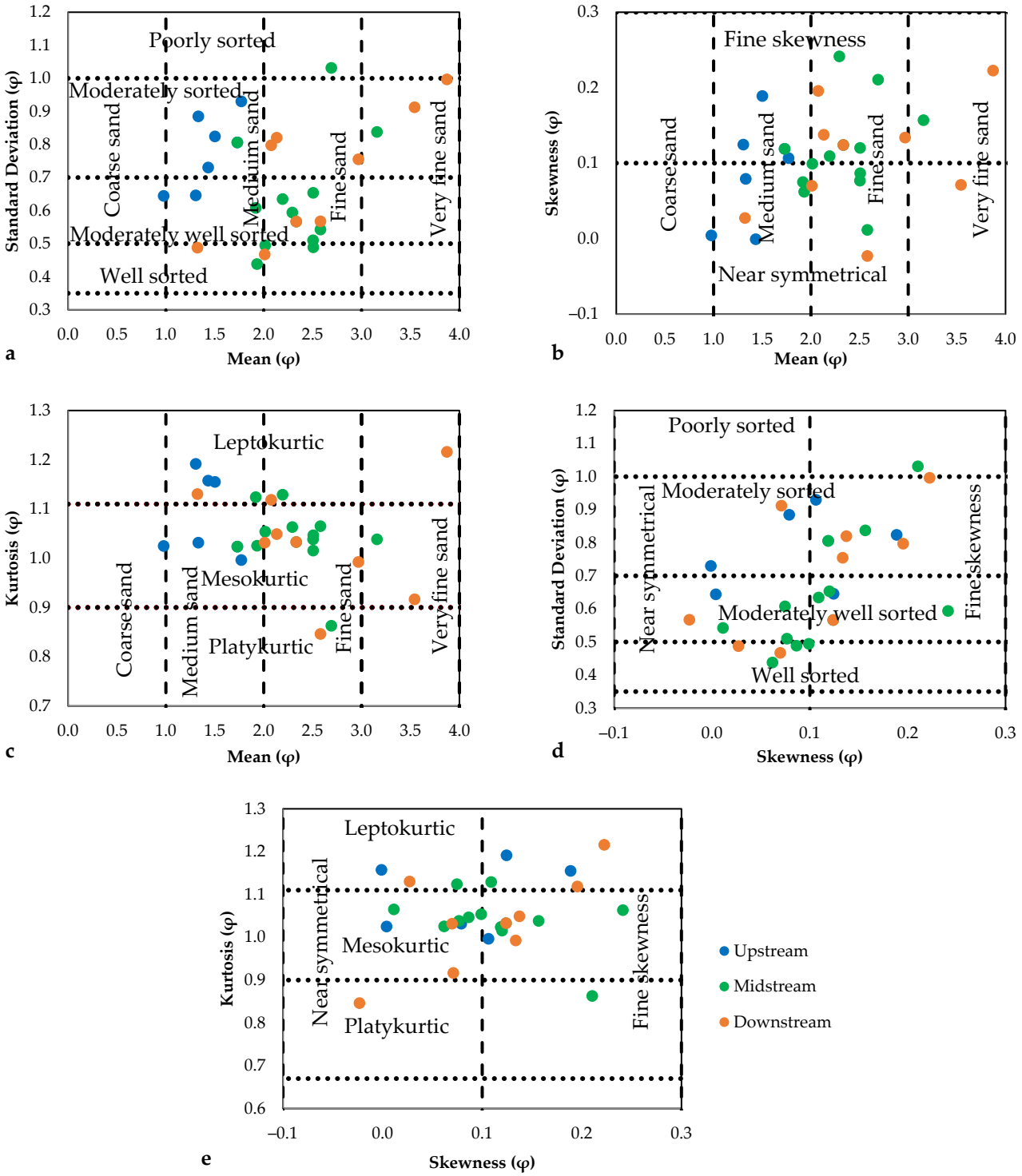

Fig. 8 Binary plots of LDFs (linear discriminant functions): (**a**) Y_1 against Y_2, (**b**) Y_2 against Y_3, and (**c**) Y_3 against Y_4.

2.7411. If Y_1 is lower than -2.7411, the environment can be defined as aeolian, while it can be defined as beach if Y_1 is higher than -2.7411.

$$Y_1 = -3.5688M_Z + 3.7016{\sigma_I}^2 - 2.0766SK + \\ +3.1135K \quad (7)$$

To distinguish between beach and shallow agitated water, the Y_2 equation can employed, with a cutoff of 65.365. The environment can be defined as shallow agitated water if Y_2 is more than 65.365, while it is beach if it is less than 65.365.

Table 4 Linear discriminant functions (LDFs) and depositional environment interpretations of the bed.

	Discriminate function				Environment of deposition			
Sample	**Y_1**	**Y_2**	**Y_3**	**Y_4**	**Y_1**	**Y_2**	**Y_3**	**Y_4**
RG1	1.19	92.81	-6.81	6.64	Aeolian	Shallow Agitated	Shallow Marine	Turbidity
RG2	0.47	78.86	-4.20	6.94	Aeolian	Shallow Agitated	Shallow Marine	Turbidity
T1	0.36	92.88	-6.38	8.19	Aeolian	Shallow Agitated	Shallow Marine	Turbidity
RG3	1.23	61.61	-3.33	5.99	Aeolian	Beach	Shallow Marine	Turbidity
T2	-0.24	104.92	-7.54	6.92	Aeolian	Shallow Agitated	Fluvial	Turbidity
RG4	0.33	72.14	-3.83	7.92	Aeolian	Shallow Agitated	Shallow Marine	Turbidity
T3	-0.84	90.84	-5.72	7.21	Aeolian	Shallow Agitated	Shallow Marine	Turbidity
RG5	-4.98	75.89	-1.75	7.83	Shallow Agitated	Shallow Agitated	Shallow Marine	Turbidity
RG6	-3.12	62.93	-1.38	7.16	Shallow Agitated	Beach	Shallow Marine	Turbidity
T4	-3.42	131.80	-9.54	7.50	Shallow Agitated	Shallow Agitated	Fluvial	Turbidity
RG7	-3.05	83.64	-3.38	8.13	Shallow Agitated	Shallow Agitated	Shallow Marine	Turbidity
T5	-4.07	83.13	-3.57	8.76	Shallow Agitated	Shallow Agitated	Shallow Marine	Turbidity
RG8	-2.14	76.46	-3.00	7.69	Aeolian	Shallow Agitated	Shallow Marine	Turbidity
RG9	-5.77	117.56	-5.96	8.55	Shallow Agitated	Shallow Agitated	Shallow Marine	Turbidity
RG10	-4.45	88.26	-3.56	7.82	Shallow Agitated	Shallow Agitated	Shallow Marine	Turbidity
T6	-4.90	76.92	-1.89	7.71	Shallow Agitated	Shallow Agitated	Shallow Marine	Turbidity
RG11	-4.83	79.65	-1.85	7.46	Shallow Agitated	Shallow Agitated	Shallow Marine	Turbidity
T7	-3.21	68.92	-2.00	7.60	Shallow Agitated	Shallow Agitated	Shallow Marine	Turbidity
RG12	-4.18	78.97	-2.70	7.86	Shallow Agitated	Shallow Agitated	Shallow Marine	Turbidity
T8	-6.82	152.37	-8.62	10.33	Shallow Agitated	Shallow Agitated	Fluvial	Fluvial
RG13	-3.30	66.15	-1.63	7.29	Shallow Agitated	Shallow Agitated	Shallow Marine	Turbidity
RG14	-5.33	76.78	-1.93	6.06	Shallow Agitated	Shallow Agitated	Shallow Marine	Turbidity
T9	-2.14	99.49	-5.91	7.74	Aeolian	Shallow Agitated	Shallow Marine	Turbidity
RG15	-6.85	128.37	-6.58	7.55	Shallow Agitated	Shallow Agitated	Shallow Marine	Turbidity
RG16	-1.98	98.52	-5.88	8.48	Aeolian	Shallow Agitated	Shallow Marine	Turbidity
GB(G1)	-0.38	57.73	-1.78	7.02	Aeolian	Beach	Shallow Marine	Turbidity
GA(G2)	-5.67	104.67	-4.75	8.06	Shallow Agitated	Shallow Agitated	Shallow Marine	Turbidity

$$Y_2 = 15.6534M_Z + 65.7091{\sigma_I}^2 + 18.1071SK + \\ +18.5043K \quad (7)$$

To distinguish between fluvial and shallow marine, the Y_3 equation can be applied, with a cutoff of -7.419. The environment can be determined as shallow marine if Y_3 is more than -7.419, while it is fluvial if it is less than -7.419.

$$Y_3 = 0.2852M_Z - 8.7604{\sigma_I}^2 - 4.8932SK + \\ +0.0482K \quad (8)$$

Finally, the Y_4 equation may be employed to distinguish between fluvial processes and turbidity current depositions. If the depositional process were affected by turbidity currents, Y_4 is supposed to be below 9.8433, while it is supposed to be controlled by fluvial processes if Y_4 is above 9.8433.

$$Y_4 = 0.7215M_Z - 0.40304{\sigma_I}^2 + 6.7322SK + \\ +5.2927K \quad (9)$$

According to the Y_1 values, all upstream samples from the study area are classified under beach processes, while the midstream and downstream are classified as aeolian (76 %) and beach (24 %) (Table 4 and Fig.8). Based on the Y_2 values, the majority (89 %) of the samples are classified as shallow marine processes. Most (89 %) of the samples are categorized as shallow marine, while the remaining (11 %) have Deltaic/Lacustrine processes based on Y_3. The majority (96 %) of the samples were placed in a turbid environment in accordance with Y_4 values. The findings of the current study demonstrate that the sediments originated from both aeolian and marine environments.

4.7. PASSEGA DIAGRAM (C-M PATTERN)

C-M plots were first presented by Passega (1957) as a method for assessing the hydrodynamic forces connected to sediment deposition. The graph shows the link between "M", which represents the median value in microns on the log probability scale, and "C", which represents the coarsest one-percentile value of the grain size distribution in microns. These parameters were chosen because the coarse sediment component better represents the depositional process than the fine fraction (1964). As shown in Figure 9, the median value (M), which was obtained from cumulative curves, was plotted against the initial percentile value (C) in microns, which represented the coarser one-percentile value. The determined transportation mode is classified as follows: N-O is rolling, O-P is bottom suspension and rolling, P-Q is rolling and suspension, Q-R is saltation, and R-S is uniform suspension.

All of the upstream samples fall into the N-O segment of type I, indicating rolling transportation

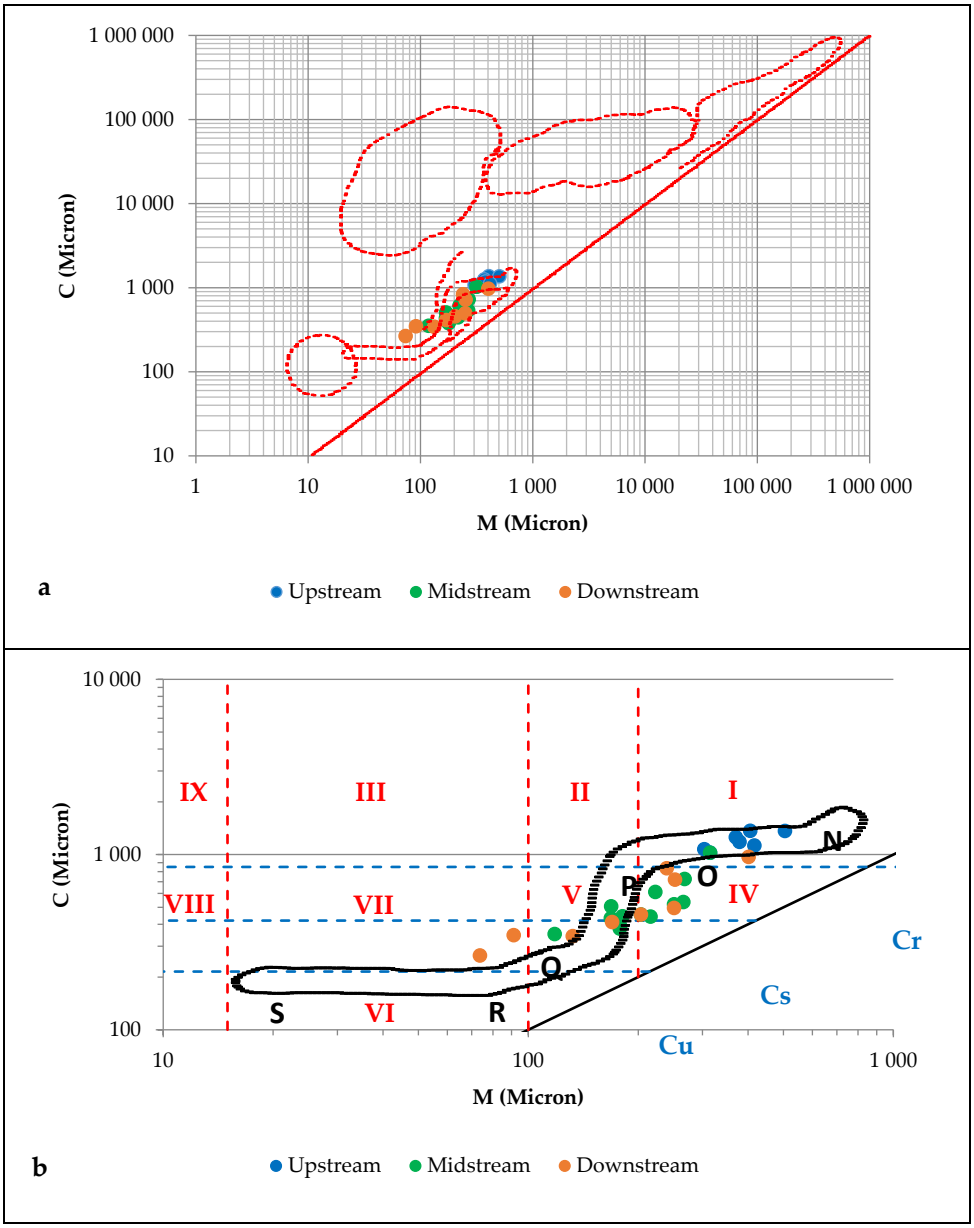

Fig. 9 A Passega diagram (C-M plot) of the Ramganga River samples (modified from Passega, 1957 and 1964) where Cr is the maximum grain size of rolling transported, Cs is the maximum grain size of graded suspension, and Cu is the maximum grain size of uniform suspension.

with no to little suspension due to their high level of coarser one-percentile and median sizes. However, all the midstream samples were transported by a higher level of suspension, with little to no rolling falling into the P-Q segment of types I and II. The majority of the downstream samples fall into the O-P and P-Q segments of types I and II, indicating transportation via suspension and rolling. This is due to their smaller particle sizes, represented by the coarser one-percentile and median sizes.

4.8. DEPOSITIONAL ENVIRONMENT

Bivariate plots of the statistical characteristics of grain size data are useful tools for determining the mechanisms of different sedimentary settings, as demonstrated by Kukal (1971) and Al-Ghadban (1990). They claim that the bivariate graphs produced by Stewart (1958), Friedman (1961), and Moiola and Weiser (1968) are important and frequently used. Friedman (1967) used scatter plots of two parameters since the values of any one parameter from multiple sedimentary contexts overlap. While not completely eliminated, the overlap was greatly reduced. The sediments were primarily associated with fluvial processes, according to the Sk vs. σ_I plot (Fig. 10a). Based on the work of Stewart (1958), Friedman (1961), and Moiola and Weiser (1968), the bivariate plot of σ_I vs. median (Fig. 10b) verifies that almost all samples fall into the domains of river and wave processes that Stewart (1958) indicated. However,

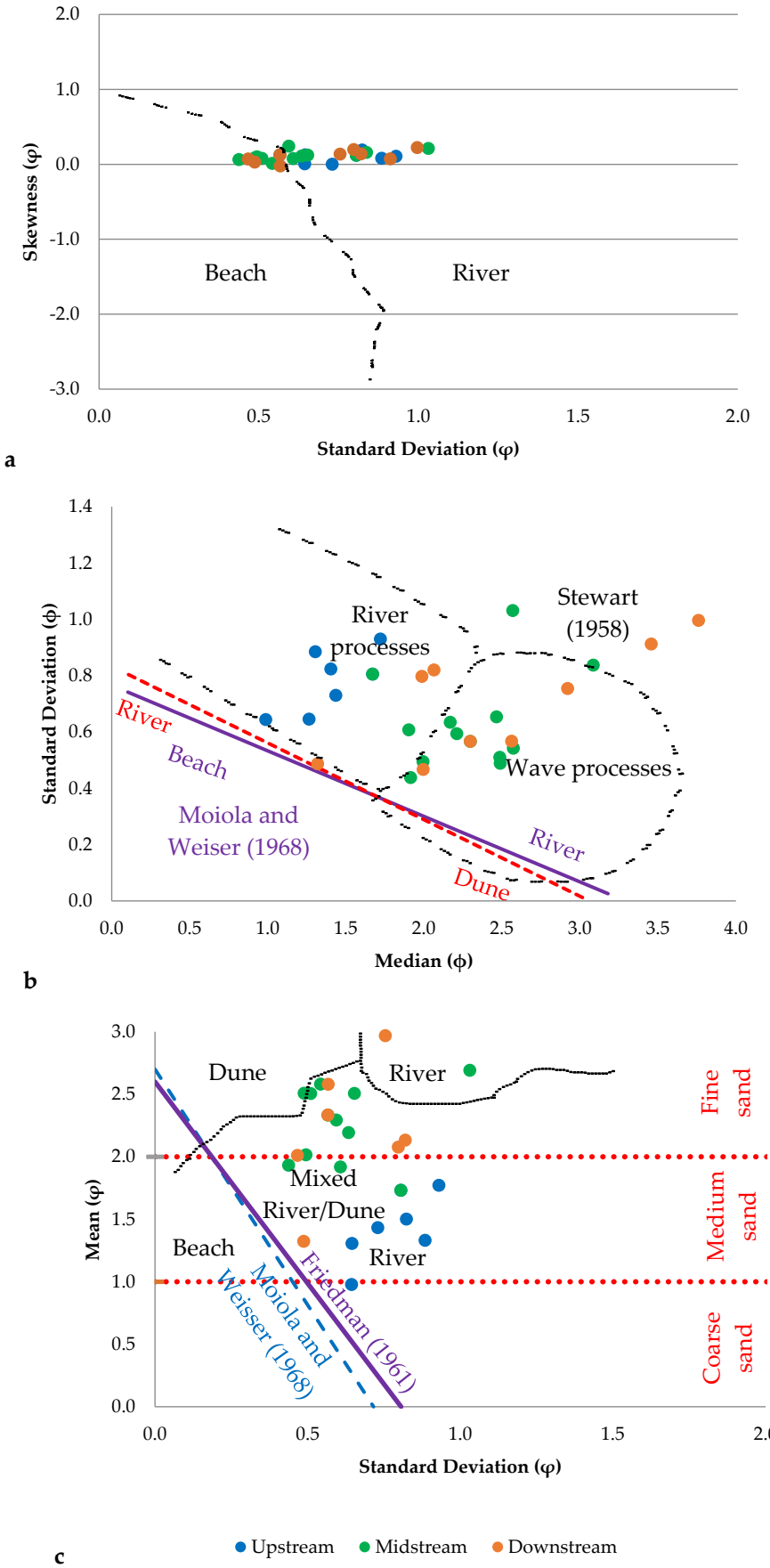

Fig. 10 A bivariant plot of **(a)** Sk versus inclusive σ_I, **(b)** inclusive σ_I versus median, and **(c)** M_Z versus inclusive σ_I, after Friedman (1961 and 1967), Stewart (1958), and Moiola and Weiser (1968).

only river and mixed river/dune sediments are included in the median vs. σ_I plots of the graphical parameters (Fig. 10c).

5. CONCLUSIONS

The Ramganga River's mainstream and tributaries were subjected to grain size analysis of twenty-seven sediment samples to investigate the regional diversity of bed sediments and their depositional environment. The main determinants of sediment load are climate, stream power, lithology, and river flow. The typical grain size measurements vary throughout the study area. The sediments being studied exhibit unimodal distributions in the upstream, midstream, and downstream regions, with only two bimodal samples in the midstream region. Using Folk's classification system, we categorized the samples into four distinct classes or facies namely: coarse sand (4 %), medium sand (33 %), fine sand (52 %), and very fine sand (11 %). The sediments found in the Ramganga River exhibit a range of mean (M_Z) values, from 0.98 (coarse sand) to 3.87 (very fine sand). The average M_Z value is 2.19, indicating fine sand. The standard deviation (σ_I) values of the samples analysed from the Ramganga River range from 0.438 (well sorted) to 1.03 (poorly sorted), with an average of 0.69 (medium to well sorted). Upstream sediments are characterized as moderately sorted medium sands, reflecting higher energy levels during deposition. In contrast, most midstream and downstream sediments are finer and better sorted, indicating lower energy levels during deposition.

The data exhibit a range of skewness (Sk) values, from -0.02 (near-symmetrical skewness) to 0.24 (fine skewness). On average, the data show an Sk value of 0.10, indicating a fine skewness. The skewness of the upstream sediments is near-symmetrical, indicating energy-level stabilization during the depositional process, while the midstream and downstream samples have a wider range, indicating changes in the energy level during the depositional process. The kurtosis (K) values span from 0.85 (indicating a platykurtic distribution) to 1.22 (indicating a leptokurtic distribution), with an average of 1.05 (indicating a mesokurtic distribution). The kurtosis of the upstream samples has a narrow range, indicating energy stabilization of the transportation medium, while the midstream and downstream samples have a wider variation, indicating a change in the energy level during the deposition process. All of the upstream samples have rolling transportation, while the majority of the midstream and downstream samples were transported by a higher level of suspension.

DATA AVAILABILITY STATEMENT

The data used in this research will be available on request.

AUTHOR CONTRIBUTIONS

Conceptualization, R.K. and M.Y.A.K.; methodology, R.K. and M.Y.A.K.; software, R.K., A.F.K., and M.Y.A.K.; validation, R.K. and M.Y.A.K.; formal analysis, M.Y.A.K.; investigation, R.K. and M.Y.A.K.; resources, M.Y.A.K.; data curation, R.K. and M.Y.A.K.; writing—original draft preparation, R.K. and M.Y.A.K.; writing—review and editing, R.K., A.F.K., and M.Y.A.K.; visualization, R.K. and M.Y.A.K.; supervision, M.Y.A.K.; project administration, R.K. and M.Y.A.K.; funding acquisition, A.F.K. All authors have read and agreed to the published version of the manuscript.

FUNDING

This project was funded by KAU Endowment (WAQF) at King Abdulaziz University, Jeddah, under grant no. WAQF: 2-135-2024. The authors, therefore, acknowledge with thanks WAQF and the Deanship of Scientific Research (DSR) for technical and financial support.

ACKNOWLEDGMENTS

This project was funded by KAU Endowment (WAQF) at King Abdulaziz University, Jeddah, under grant no. WAQF: 2-135-2024. The authors, therefore, acknowledge with thanks WAQF and the Deanship of Scientific Research (DSR) for technical and financial support.

CONFLICTS OF INTEREST

The authors declare no conflicts of interest.

REFERENCES

Ahamad, M.I., Yao, Z., Ren, L., Zhang, C., Li, T., Lu, H., ... and Feng, W.: 2024, Impact of heavy metals on aquatic life and human health: a case study of River Ravi Pakistan. Front. Mar. Sci., 11, 1374835. DOI: 10.3389/fmars.2024.1374835

Al-Ghadban, A.N.: 1990, Holocene sediments in a shallow bay, southern coast of Kuwait, Arabian Gulf. Mar. Geol., 92, 3-4, 237–254. DOI: 10.1016/0025-3227(90)90006-6

Baiyegunhi, C., Liu, K. and Gwavava, O.: 2017, Grain size statistics and depositional pattern of the Ecca Group sandstones, Karoo Supergroup in the Eastern Cape Province, South Africa. Open Geosci., 9, 1, 554–576. Top of Form Bottom of Form. DOI: 10.1515/geo-2017-0042

Boggs, S.: 2006, Principles of sedimentology and stratigraphy. 4th Edition, Pearson Education Inc., Upper Saddle River, 662 pp.

Boggs, S.: 2009, Petrology of sedimentary rocks. Cambridge University Press, 600 pp.

Boggs, S.: 2012, Principles of sedimentology and stratigraphy. Pearson, London.

Chakrapani, G.J.: 2005, Major and trace element geochemistry in upper Ganga River in the Himalayas, India. Environ. Geol., 48, 189–201. DOI: 10.1007/s00254-005-1287-1

Chakrapani, G.J. and Saini, R.K.: 2009, Temporal and spatial variations in water discharge and sediment load in the Alaknanda and Bhagirathi Rivers in Himalaya, India. J. Asian Earth Sci., 35, 6, 545–553. DOI: 10.1016/j.jseaes.2009.04.002

Chalov, S., Prokopeva, K., Magritsky, D., Grigoriev, V., Fingert, E., Habel, M., Juhls, B., Morgenstern, A., Overduin, P.P. and Kasimov, N.: 2023, Climate change impacts on streamflow, sediment load and carbon fluxes in the Lena River delta. Ecol. Indic., 157, 111252. DOI: 10.1016/j.ecolind.2023.111252

CWC: 2012, Environmental evaluation study of Ramganga Major Irrigation Project. Central Water Commission, Uttar Pradesh, India, 1, 16 pp.

Daityari, S. and Khan, M.Y.A.: 2017, Temporal and spatial variations in the engineering properties of the sediments in Ramganga River, Ganga Basin, India. Arab. J. Geosci., 10, 1–13. DOI: 10.1007/s12517-017-2915-2

Dawson, M.: 1988, Sediment size variation in a braided reach of the Sunwapta River, Alberta, Canada. Earth Surf. Process. Landf., 13, 7, 599–618. DOI: 10.1002/esp.3290130705

Feng, J.L., Hu, Z.G., Ju, J.T. and Zhu, L.P.: 2011, Variations in trace element (including rare earth element) concentrations with grain sizes in loess and their implications for tracing the provenance of eolian deposits. Quat. Int., 236, 1-2, 116–126. DOI: 10.1016/j.quaint.2010.04.024

Folk, R.L.: 1966, A review of grain-size parameters. Sedimentology, 6, 2, 73-93.

Folk, R.L.: 1980, Petrology of sedimentary rocks. Hemphill Pub. Co.

Folk, R.L. and Ward, W.C.: 1957, Brazos River bar [Texas]; a study in the significance of grain size parameters. J. Sediment. Res., 27, 1, 3–26.

Friedman, G.M.: 1961, Distinction between dune, beach, and river sands from their textural characteristics. J. Sediment. Res., 31, 4, 514–529. DOI: 10.1306/74D70BCD-2B21-11D7-8648000102C1865D

Friedman, G.M.: 1967, Dynamic processes and statistical parameters compared for size frequency distribution of beach and river sands. J. Sediment. Res., 37, 2, 327–354. DOI: 10.1306/74D716CC-2B21-11D7-8648000102C1865D

Gaillardet, J., Dupré, B. and Allègre, C.J.: 1999, Geochemistry of large river suspended sediments: silicate weathering or recycling tracer? Geochim. Cosmochim. Acta, 63, 23-24, 4037–4051. DOI: 10.1016/S0016-7037(99)00307-5

Goni, M.A., Monacci, N., Gisewhite, R., Ogston, A., Crockett, J. and Nittrouer, C.: 2006, Distribution and sources of particulate organic matter in the water column and sediments of the Fly River Delta, Gulf of Papua (Papua New Guinea). Estuar. Coast. Shelf Sci., 69, 1-2, 225–245. DOI: 10.1016/j.ecss.2006.04.012

Gupta, R.P. and Joshi, B.C.: 1990, Landslide hazard zoning using the GIS approach - a case study from the Ramganga catchment, Himalayas. Eng. Geol., 28, 1-2, 119–131. DOI: 10.1016/0013-7952(90)90037-2

Hakro, A.A., Xiao, W., Mastoi, A.S., Yan, Z., Samtio, M.S. and Rajper, R.H.: 2021, Grain size analysis of the Oligocene Nari Formation sandstone in the Laki Range, southern Indus Basin, Pakistan: Implications for depositional setting. Geol. J., 56, 11, 5440–5451. DOI: 10.1002/gj.4251

Joshua, E.O. and Oyebanjo, O.A.: 2010, Grain-size and heavy mineral analysis of River Osun sediments. Aust. J. Basic Appl. Sci., 4, 3, 498–501.

Khan, A.U. and Rawat, B.P.: 1992, Quaternary geology and geomorphology of a part of Ganga basin in parts of Bareilly, Badaun, Shahjahanpur and Pilibhit district, Uttar Pradesh. Rec. Geol. Surv. India, 125, 8, 41-43.

Khan, M.Y.A.: 2025, Regional ANN model for estimating missing daily suspended sediment load in complex, heterogeneous catchments. J. Geochem. Explor., 269, 107643. DOI: 10.1016/j.gexplo.2024.107643

Khan, M.Y.A., Daityari, S. and Chakrapani, G.J.: 2016a, Factors responsible for temporal and spatial variations in water and sediment discharge in Ramganga River, Ganga Basin, India. Environ. Earth Sci., 75, 4, 283. DOI: 10.1007/s12665-015-5148-2

Khan, M.Y.A., Gani, K.M. and Chakrapani, G.J.: 2016b, Assessment of surface water quality and its spatial variation. A case study of Ramganga River, Ganga Basin, India. Arab. J. Geosc., 9, 1, 28. DOI: 10.1007/s12517-015-2134-7

Khan, M.Y.A., Gani, K.M. and Chakrapani, G.J.: 2017, Spatial and temporal variations of physicochemical and heavy metal pollution in Ramganga River - a tributary of River Ganges, India. Environ. Earth Sci., 76, 1–13. DOI: 10.1007/s12665-017-6547-3

Khan, M.Y.A., Hasan, F. and Tian, F.: 2019, Estimation of suspended sediment load using three neural network algorithms in Ramganga River catchment of Ganga Basin, India. Sustain. Water Resour. Manag., 5, 1115–1131. DOI: 10.1007/s40899-018-0288-7

Khan, M.Y.A., Hasan, F., Panwar, S. and Chakrapani, G.J.: 2016c, Neural network model for discharge and water-level prediction for Ramganga River catchment of Ganga Basin, India. Hydrol. Sci. J., 61, 11, 2084–2095. DOI: 10.1080/02626667.2015.1083650

Khan, M.Y.A., Hu, H., Tian, F. and Wen, J.: 2020, Monitoring the spatio-temporal impact of small tributaries on the hydrochemical characteristics of Ramganga River, Ganges Basin, India. Int. J. River Basin Manag., 18, 2, 231–241. DOI: 10.1080/15715124.2019.1675677

Kido, R., Inoue, T., Hatono, M. and Yamanoi, K.: 2023 Assessing the impact of climate change on sediment discharge using a large ensemble rainfall dataset in Pekerebetsu River basin, Hokkaido. Prog. Earth Planet. Sci., 10, 1, 54. DOI: 10.1186/s40645-023-00580-0

Knighton, A.D.: 1980, Longitudinal changes in size and sorting of stream-bed material in four English rivers. Geol. Soc. Am. Bull., 91, 1, 55–62. DOI: 10.1130/0016-7606(1980)91

Krumbein, W.C. and Monk, G.D.: 1943, Permeability as a function of the size parameters of unconsolidated sand. Trans. AIME, 151, 1, 153–163. DOI: 10.2118/943153-G

Kukal, Z.: 1971, Geology of Recent Sediments. Academic Press, London, 409 pp.

Lindholm, R.: 1987, A practical approach to sedimentology. Allen and Unwin, London, 278 pp.

Milliman, J.D. and Meade, R.H.: 1983, World-wide delivery of river sediment to the oceans. J. Geol., 91, 1, 1–21. DOI: 10.1086/628741

Moiola, R.J. and Weiser, D.A.N.I.E.L.: 1968, Textural parameters; an evaluation. J. Sediment. Res., 38, 1, 45–53. DOI: 10.1306/74D718C5-2B21-11D7-8648000102C1865D

Mueller, E.R. and Pitlick, J.: 2013, Sediment supply and channel morphology in mountain river systems: 1. Relative importance of lithology, topography, and climate. J. Geophys. Res., Earth Surface, 118, 4, 2325–2342. DOI: 10.1002/2013JF002843

Mukherjee, R. and Deb, P.: 2024, Application of GIS-based analytical hierarchy process for assessment and mapping of flood risk zone in the lower Ramganga River Basin, Western Gangetic Plain, India. Environ. Dev. Sustain., 26, 3, 6163–6193. DOI: 10.1007/s10668-023-02957-z

Nwineewii, J.D., Edori, O.S. and Onuchukwu, P.U.G.: 2018, Concentration, ecological risk and enrichment factor assessment of selected heavy metals in sediments from New Calabar River, Nigeria. J. Appl. Sci. Environ. Manag., 22, 10, 1643–1647. DOI: 10.4314/jasem.v22i10.20

Pandey, S.K., Singh, A.K. and Hasnain, S.I.: 2002, Grain-size distribution, morphoscopy and elemental chemistry of suspended sediments of Pindari Glacier, Kumaon Himalaya, India. Hydrol. Sci. J., 47, 2, 213–226. DOI: 10.1080/02626660209492925

Panwar, S., Khan, M.Y.A., Alharbi, M.O.H., Pande, C.B. and ElKashouty, M.: 2024, Control of antropogenic factors on the dissolved carbon sources in the Ramganga River, Ganga Basin, India. Earth Syst. Environ., 1–11. DOI: 10.1007/s41748-024-00417-w

Panwar, S., Yang, S., Srivastava, P., Khan, M.Y.A., Sangode, S.J. and Chakrapani, G.J.: 2020, Environmental magnetic characterization of the Alaknandaa and Ramganga river sediments, Ganga basin, India. Catena, 190, 104529. DOI: 10.1016/j.catena.2020.104529

Passega, R.: 1957, Texture as characteristic of clastic deposition. AAPG Bull., 41, 9, 1952–1984. DOI: 10.1306/0BDA594E-16BD-11D7-8645000102C1865D

Passega, R.: 1964, Grain size representation by CM patterns as a geologic tool. J. Sediment. Res., 34, 4, 830–847. DOI: 10.1306/74D711A4-2B21-11D7-8648000102C1865D

Pindi, S. and Jayakumar, K.V.: 2023, Assessment of sedimentation status and trap efficiency of Wyra reservoir. J. Hydraul. Eng., 29, 5, 632–641. DOI: 10.1080/09715010.2022.2122879

Pizzuto, J.E.: 1995, Downstream fining in a network of gravel-bedded rivers. Water Resour. Res., 31, 3, 753–759. DOI: 10.1029/94WR02532

Ramanathan, A.L., Rajkumar, K., Majumdar, J., Singh, G., Behera, P.N., Santra, S.C. and Chidambaram, S.: 2009, Textural characteristics of the surface sediments of a tropical mangrove Sundarban ecosystem India. Indian J. Geo-Mar. Sci., 38, 397–403.

Ranjan, R. and Mishra, A.: 2023, Climate change impact on streamflow and suspended sediment load in the flood-prone river basin. J. Water Clim. Change, 14, 7, 2260–2276. DOI: 10.2166/wcc.2023.037

Ren, Z., Wang, T., Wang, Y., and Qu, S.: 2018, A study on the characteristics and influencing factors of reservoir sedimentation in Wanjiazhai Reservoir. In: MATEC Web of Conferences, 246, 01046. EDP Sciences.

Rice, S.: 1994, Towards a model of changes in bed material texture at the drainage basin scale. Process Models and Theoretical Geomorphology, 159–172.

Sahu, B.K.: 1964, Depositional mechanisms from the size analysis of clastic sediments. J. Sediment. Res., 34, 1, 73–83. DOI: 10.1306/74D70FCE-2B21-11D7-8648000102C1865D

Sarkar, S.K., Bhattacharya, A. and Bhattacharya, B.: 2003, The river Ganga of northern India: an appraisal of its geomorphic and ecological changes. Water Sci. Technol., 48, 7, 121–128. DOI: 10.2166/wst.2003.0432

Singh, I.B.: 1996, Geological evolution of Ganga Plain-an overview. J. Palaeontol. Soc. India, 41, 1, 99–137. DOI: 10.1177/0971102319960113

Singh, M., Singh, I.B. and Müller, G.: 2007, Sediment characteristics and transportation dynamics of the Ganga River. Geomorphology, 86, 1-2, 144–175. DOI: 10.1016/j.geomorph.2006.08.011

Slattery, M.C. and Burt, T.P.: 1997, Particle size characteristics of suspended sediment in hillslope runoff and stream flow. Earth Surf. Process. Landf., 22, 8, 705–719. DOI: 10.1002/(SICI)1096-9837(199708)22:8

Sok, T., Oeurng, C., Ich, I., Sauvage, S. and Miguel Sánchez-Pérez, J.: 2020, Assessment of hydrology and sediment yield in the Mekong River Basin using SWAT model. Water, 12, 12, 3503. DOI: 10.3390/w12123503

Stewart Jr, H.B.: 1958, Sedimentary reflections of depositional environment in San Miguel lagoon, Baja California, Mexico. AAPG Bull., 42, 11, 2567–2618. DOI: 10.1306/0BDA5BFA-16BD-11D7-8645000102C1865D

Tinoco, R.O. and Coco, G.: 2018, Turbulence as the main driver of resuspension in oscillatory flow through vegetation. J. Geophys. Res., Earth Surface, 123, 5, 891–904. DOI: 10.1002/2017JF004504

Valdiya, K.S.: 1980, Geology of Kumaun lesser Himalaya.

Visher, G.S.: 1969, Grain size distributions and depositional processes. J. Sediment. Res., 39, 3. DOI: 10.1306/74D71D9D-2B21-11D7-8648000102C1865D

Walling, D.E.: 2005, Tracing suspended sediment sources in catchments and river systems. Sci. Total Environ., 344, 1-3, 159–184. DOI: 10.1016/j.scitotenv.2005.02.011

Wang, Y.M., Traore, S. and Kerh, T.: 2008, Monitoring event-based suspended sediment concentration by artificial neural network models. WSEAS Trans. Comput., 5, 7, 359–368. DOI: 10.5555/1457927.1457947

Warren, N., Allan, I.J., Carter, J.E., House, W.A. and Parker, A.: 2003, Pesticides and other micro-organic contaminants in freshwater sedimentary environments - a review. Appl. Geochem., 18, 2, 159–194. DOI: 10.1016/S0883-2927(02)00159-2

Weltje, G.J. and von Eynatten, H.: 2004, Quantitative provenance analysis of sediments: review and outlook. Sediment. Geol., 171, 1-4, 1–11. DOI: 10.1016/j.sedgeo.2004.05.007

Xu, J.: 2000, Grain-size characteristics of suspended sediment in the Yellow River, China. Catena, 38, 3, 243–263. DOI: 10.1016/S0341-8162(99)00070-3

Xu, Y., Song, J., Duan, L., Li, X., Yuan, H., Li, N., ... and Yin, X.: 2012, Fraction characteristics of rare earth elements in the surface sediment of Bohai Bay, North China. Environ. Monit. Assess., 184, 7275–7292. DOI: 10.1007/s10661-011-2496-6

Yadav, A., Singh, R.M., Pandey, M.K., Maurya, S.P. and Singh, S.K.: 2024, Hydrodynamic modelling of river training works for protection of group of villages on the left bank of Ramganga River: a case study. Nat. Hazards, 1–16. DOI: 10.1007/s11069-024-06888-4

Yang, H. and Shi, C.: 2019, Sediment grain-size characteristics and its sources of ten wind-water coupled erosion tributaries (the Ten Kongduis) in the Upper Yellow River. Water, 11, 1, 115. DOI: 10.3390/w11010115

Zamroni, A., Putra, B.P. and Prasetya, H.N.E.: 2020, Anthropogenic influences on morphological changes in the Progo River, Daerah Istimewa Yogyakarta Province, Indonesia. Sustinere J. Environ. Sustain., 4, 3, 205–223. DOI: 10.22515/sustinere.jes.v4i3.119

Zhang, J., Lei, J., Huai, W. and Nepf, H.: 2020, Turbulence and particle deposition under steady flow along a submerged seagrass meadow. J. Geophys. Res., Oceans, 125, 5, e2019JC015985. DOI: 10.1029/2019JC015985

Zhang, Q., Xu, C.Y., Becker, S. and Jiang, T.: 2006, Sediment and runoff changes in the Yangtze River basin during past 50 years. J. Hydrol., 331, 3-4, 511–523. DOI: 10.1016/j.jhydrol.2006.05.036

APPENDIX

Table A1 The geographic coordinates of the collected samples from the Ramganga River.

Region	Sample ID	Elevation (m)	Longitude	Latitude
Upstream	RG1	1,304	79.32158	29.98402
	RG2	878	79.25544	29.73223
	T1	738	79.26808	29.69157
	RG3	811	79.26115	29.69679
	T2	544	79.09628	29.60969
	RG4	531	79.09361	29.60605
	T3	345	79.00761	29.58610
Midstream	RG5	259	78.76117	29.49664
	RG6	207	78.63611	29.31443
	T4	214	78.54740	29.32115
	RG7	205	78.64934	29.24335
	T5	232	78.79273	29.30472
	RG8	203	78.67908	29.12716
	RG9	185	78.69839	29.06814
	RG10	180	78.74411	28.89064
	T6	190	78.81061	28.93236
	RG11	157	78.91203	28.66856
	T7	167	78.98742	28.78525
	RG12	154	79.22953	28.44992
Downstream	T8	148	79.28208	28.46558
	RG13	150	79.36803	28.29472
	RG14	139	79.51386	28.09422
	T9	141	79.63703	28.07069
	RG15	139	79.62331	27.68199
	RG16	123	79.69754	27.49798
	GB(G1)	112	79.62953	27.39792
	GA(G2)	107	79.88306	27.14978

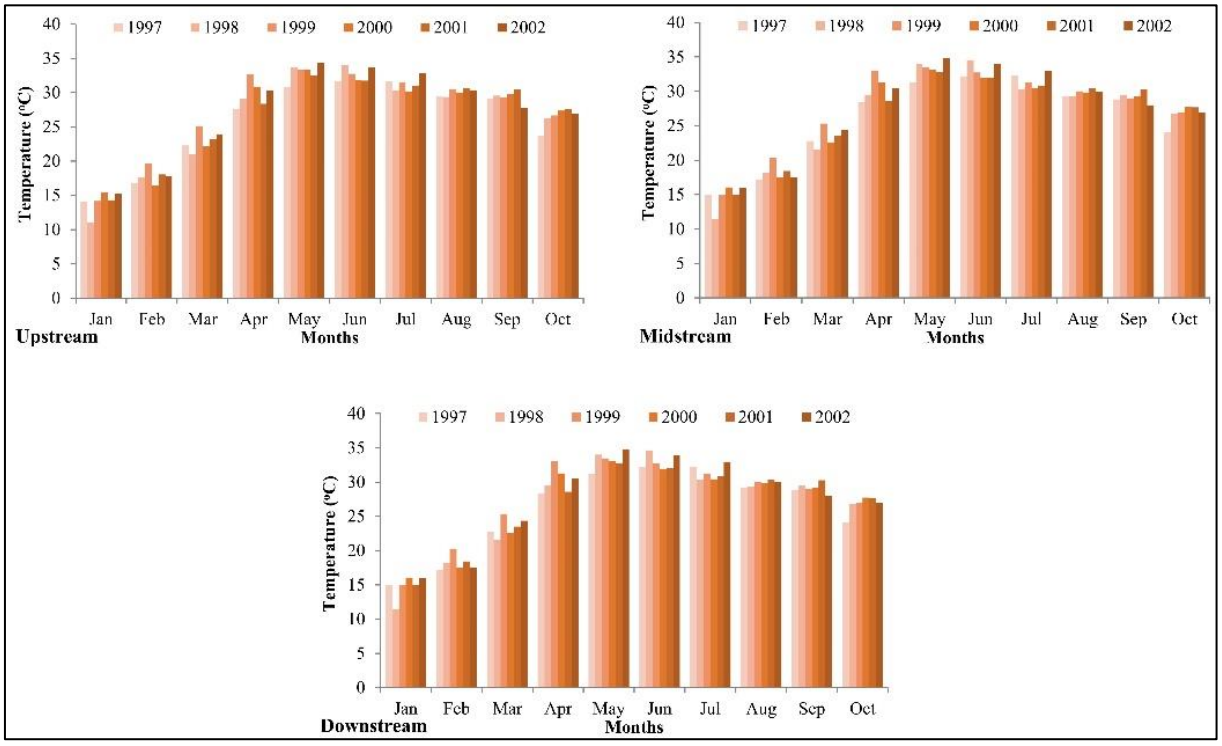

Fig. A1 Average monthly temperature in upstream, midstream, and downstream regions of Ramganga River.

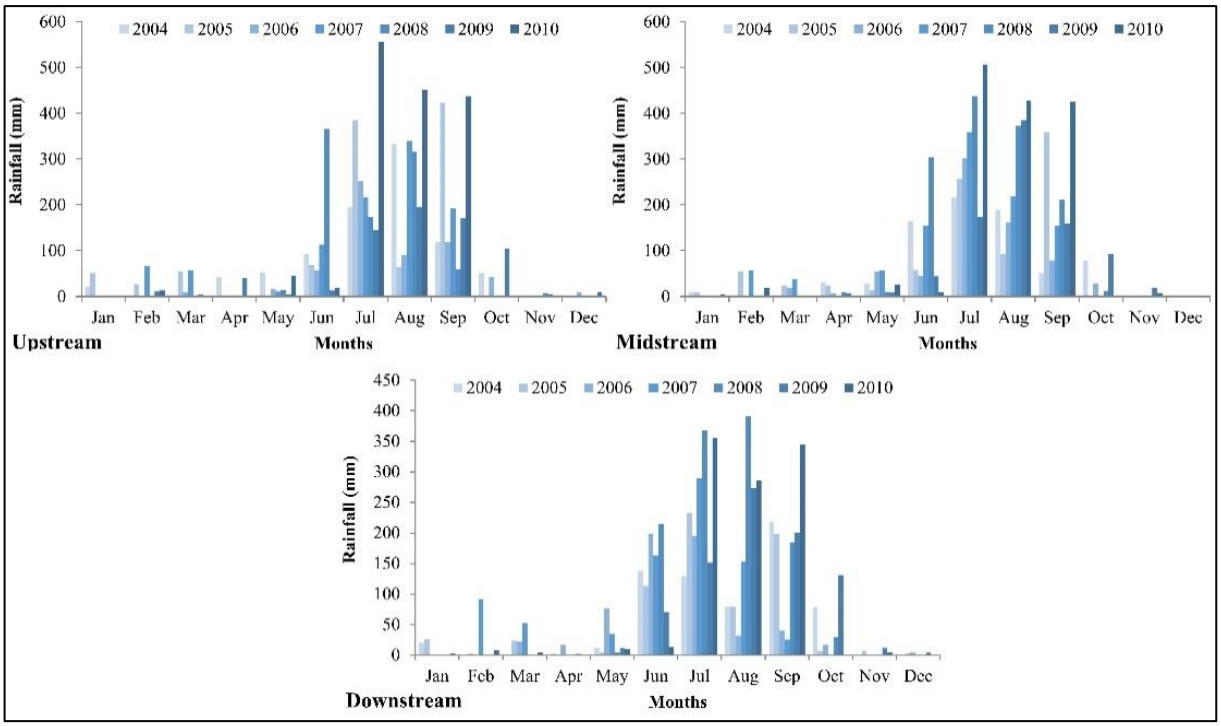

Fig. A2 Average monthly rainfall in upstream, midstream, and downstream regions of Ramganga River.

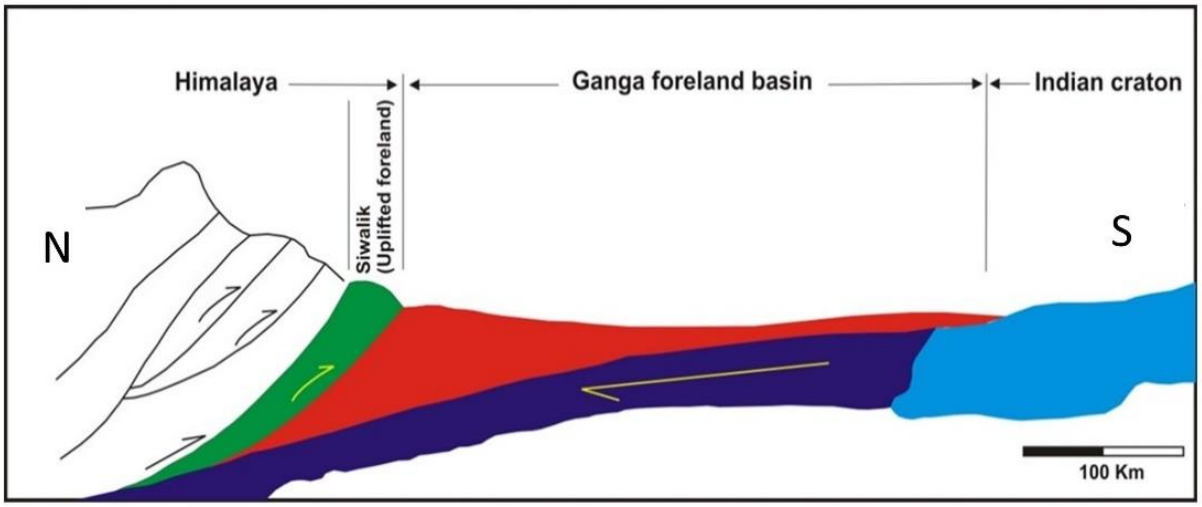

Fig. A3 Schematic cross-section of the Ganga Foreland Basin (modified after Singh, 1996).

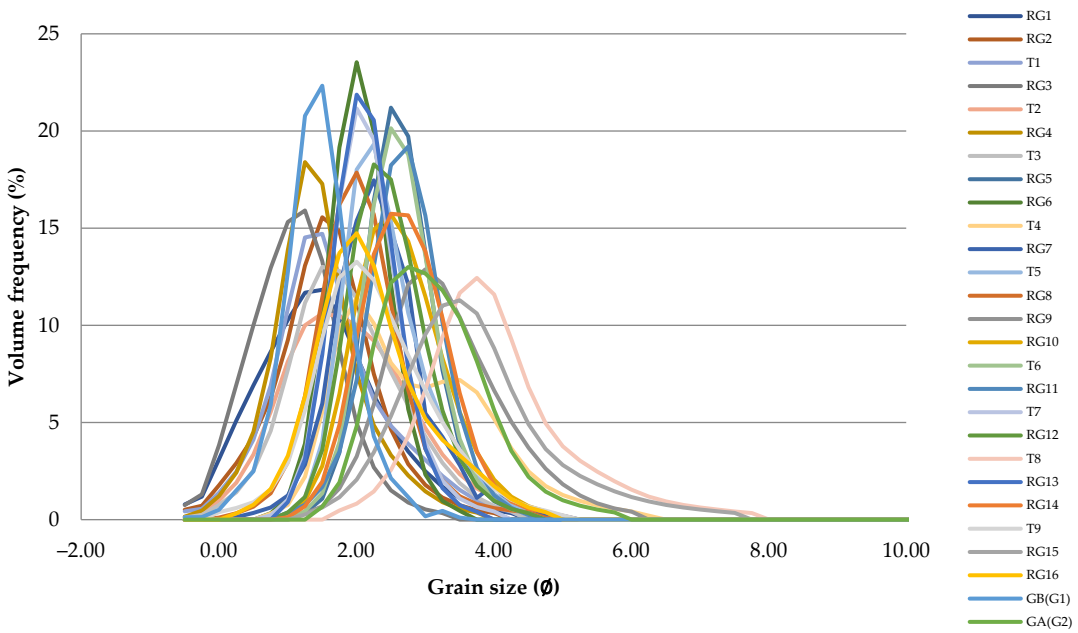

Fig. A4 Volume percentage plots of the Ramganga River samples.

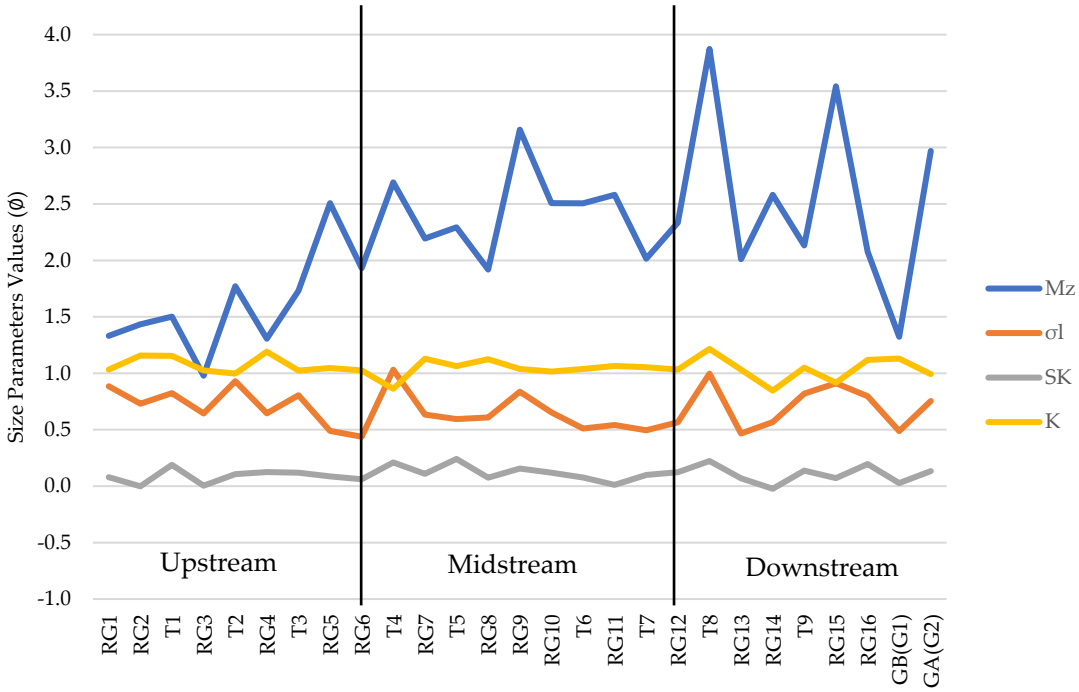

Fig. A5 Lateral variation in the Ramganga River samples.